Recognizing Sitting Activities of Excavator Operators Using Multi-Sensor Data Fusion with Machine Learning and Deep Learning Algorithms

Jue Li [a, *], Gaotong Chen [a], Maxwell Fordjour Antwi-Afari [b]

[a] *School of Economics and Management, China University of Geosciences, Wuhan, Hubei, China*

[b] *Department of Civil Engineering, College of Engineering and Physical Sciences, Aston University, Birmingham, UK*

[*] Corresponding author at: School of Economics and Management, China University of Geosciences, Wuhan, Hubei, China. *E-mail address*: jueli0824@gmail.com

Abstract

Recognizing excavator operators' sitting activities is crucial for improving their health, safety, and productivity. Moreover, it provides essential information for comprehending operators' behavior patterns and their interaction with construction equipment. However, limited research has been conducted on recognizing excavator operators' sitting activities. This paper presents a method for recognizing excavator operators' sitting activities by leveraging multi-sensor data and employing machine learning and deep learning algorithms. A multi-sensor system integrating interface pressure sensor arrays and inertial measurement units was developed to capture excavator operators' sitting activity information at a real construction site. Results suggest that the gated recurrent unit achieved outstanding performance, with 98.50% accuracy for static sitting postures and 94.25% accuracy for compound sitting actions. Moreover, several multi-sensor combination schemes were proposed to strike a balance between practicability and recognition accuracy. These findings demonstrate the feasibility and potential of the proposed approach for recognizing operators' sitting activities on construction sites.

Keywords: Excavator operator; Sitting activity recognition; Multi-sensor fusion; Machine learning; Deep learning; Interface pressure

1. Introduction

Construction equipment operation plays a vital role on construction sites, relying heavily on the expertise and efficiency of construction equipment operators. These operators bear the responsibility of operating a wide range of machinery, such as excavators, cranes, bulldozers, and forklifts, which are indispensable for ensuring the safe and effective completion of construction projects. Throughout the operation of construction equipment, the activities performed by operators dominate the operational process and affect various aspects of construction task performance [1]. These activities encompass a diverse range of body postures and compound movements carried out by the

operator while seated, playing a crucial role in their daily tasks [2-5]. Operators often spend prolonged durations operating construction equipment in harsh environments and are often subjected to conditions that pose significant construction risks [2-5]. Notably, operators' sitting activities have been demonstrated to possess profound implications for construction performance, including operational safety [6,7], workers' health [2,3,8,9], and production efficiency [10]. Moreover, human body activities serve as fundamental elements reflecting human behaviors during interactions with the environment [11]. With the growing presence of machinery operations with varying levels of automation at modern construction sites [12], continuous monitoring of operators' sitting activities has become increasingly necessary. Such monitoring provides essential information for modeling and analyzing operators' daily operational performance and behavioral patterns, thereby offering insights for understanding human-machine interactions context at the construction sites. Therefore, given the strong relationship between sitting activities and construction equipment operation performance, it becomes evident that recognizing operators' sitting activities is of substantial necessity and practical significance.

Research on activity recognition of construction workers has received considerable attention. Existing methods for recognizing workers' activities can be categorized into three main groups: kinematic-based, computer vision-based, and audio-based methods [13,14]. These methods capture relevant information from multiple modalities of workers' activities and have been applied individually or in combination to address activity recognition challenges in several application scenarios [13-15], such as work-related musculoskeletal disorders (WMSDs) and operational safety risk assessment and productivity analysis. While extant studies on construction workers' activity recognition mainly focus on manual operation tasks, specific research focusing on recognizing sitting activities of construction equipment operators remains limited. Construction equipment operation scenes, predominantly involving sitting activities, differ significantly from manual construction work settings. This presents challenges when attempting to apply existing activity recognition methods designed for manual tasks to the recognition of sitting activities performed by construction equipment operators. On the one hand, operators' sitting activities primarily involve restricted body movements within a confined space. The movements of the operator's arms and torso are minimal, making it challenging to identify changes in sitting posture solely through the image information obtained from cameras placed in the equipment cockpit [13,16]. On the other hand, the perception of sitting activities is influenced by factors such

as the cockpit's optics, acoustic environment, and vibration, which introduce difficulties in sensor placement and data collection [17]. In particular, vibrations and self-motion of construction equipment produce irregular noise signals that can affect the performance of kinematic-based sensors, such as accelerometers, thus reducing recognition performance. Taking the above into account, there exists a distinct research gap that needs to be addressed to develop an effective method for recognizing the sitting activities of construction equipment operators at real construction sites.

In broader occupational and daily life scenarios, various techniques for sitting activity recognition have been developed [18-22]. In addition to the aforementioned techniques, the interface pressure sensing technique has emerged as a promising approach and has been applied in various sectors, such as office environments [23-26], medical health [27], and car driving [28]. This technique enables accurate recognition of the pressure exerted on the interface between the human and the seat, providing necessary data that can inform ergonomic interventions and policy development [29]. Compared with kinematic-based and computer vision-based methods, interface pressure sensing technology is less invasive and can sensitively capture small pressure changes during sitting activities, which could be beneficial to obtain high recognition performance while achieving good practicability on construction sites [30]. These characteristics give this technology a natural advantage when applied to sitting activity recognition. Therefore, this paper adopts a low-cost and easy-to-install interface pressure sensing technology to collect excavator operators' sitting activity-related data. However, implementing the interface pressure sensing technique alone may not be sufficient to effectively address sitting activity recognition in construction equipment operation contexts. The vibration and movement of construction equipment can cause changes in the interface pressure between operators and their seats. Consequently, the collected pressure data is insufficient to directly reflect changes in operators' actual sitting postures and compound movements during dynamic operation scenarios. Given the complexity of operators' sitting activity recognition, recent studies have utilized multiple homogeneous or heterogeneous sensors to obtain more information, combined with machine learning or deep learning algorithms to improve activity recognition performance [31-34]. Nevertheless, the sensors placement, indicators, and features proposed in previous studies may not be applicable to construction equipment operation scenarios. Thus, further exploration is necessary to identify suitable combinations of multiple sensors and corresponding features for recognizing operators' sitting activities, while considering both practicability and recognition performance, which are crucial for construction practice [35-

37].

To this end, this paper presents a multi-sensor fusion-based method for recognizing excavator operators' sitting activities using machine learning and deep learning algorithms. To address the limitations of relying solely on interface pressure sensing technology in construction equipment operation scenarios, a multi-sensor system integrating two interface pressure sensor arrays and four inertial measurement units (IMUs) was developed. The IMUs were arranged on both the operator's body and construction equipment to supplementarily collect the data on operators' body movement and synchronized equipment vibration and motion. A sitting activity classification system including static sitting postures and compound sitting actions was constructed to capture the full range of operators' sitting activities. Several indicators related to the operators' sitting activities were established based on the existing studies. Commonly used supervised machine learning and deep learning algorithms for construction workers' activity recognition were applied. To demonstrate the feasibility of the proposed method, a field experiment was conducted at a real excavator operation site to collect data reflecting the problem characteristics. Several multi-sensor combination schemes were developed considering various potential application scenarios in earthmoving tasks. By comparing the performance of these algorithms across different schemes, methods that exhibit practicability (e.g., cost, invasiveness, and ease of deployment) or high recognition performance were investigated. The results underscore the effectiveness of combined multi-sensor and machine/deep learning algorithms for recognizing operators' sitting activities within the context of excavator operations. Additionally, the findings provide a preliminary demonstration of the feasibility and application value of the proposed approach in a broader range of construction equipment operation environments.

2. Literature review

2.1. Activity recognition of construction workers

Monitoring construction workers' activities is critical to ensuring their health [2,38], safety risks [1], and tracking the productivity of construction projects [13,14]. Since nearly 80% of fatal and non-fatal injuries are caused by unsafe behaviors on construction sites [39], and when workers repeatedly perform weight-bearing, kneeling, and twisting tasks attributed to awkward working postures [40], they are at risk of suffering long-term ergonomic injuries or

WMSDs [41]. Consequently, workers' activity recognition can provide necessary data and information for health and safety management. Such recognition systems offer capabilities to detect target activities (e.g., awkward posture, inappropriate operations, etc.) and reduce associated health and safety risks [42-44]. Moreover, activity recognition is widely utilized for measuring the time spent on specific activities, assessing working efficiency, and analyzing workers' activity levels to identify areas for productivity improvement [45]. Therefore, health assurance, safety risk assessment, and productivity analysis are considered primary research objectives in the field of activity recognition [46], rendering it an essential task at construction sites.

Over the past decades, the recognition of worker activity has primarily relied on self-reported or observational methods [47,48]. While these traditional methods are simple and less expensive, they often prove labor-intensive, time-consuming, and less accurate [49]. With advancements in sensing technologies, researchers have increasingly shifted towards real-time monitoring of workers' activity [50], incorporating various sensing technologies and classification algorithms using machine learning or deep learning [13,14]. As mentioned above, workers' activity recognition methods can be divided into three main categories based on sensing technologies. Among them, kinematic-based methods typically employ wearable sensors such as IMUs, physiological sensors, and insole pressure sensors to collect time-series data to identify kinematic patterns associated with workers' activities [51-54]. These methods offer low-cost and automated data acquisition, but are often intrusive to users and impact their working performance [14]. Computer vision-based approach utilizes 2D image/video cameras and 3D range cameras to capture visual data on workers' activities for recognition [55]. These methods generally provide less intrusive data acquisition capabilities, but they tend to be limited by ambient visibility and raise privacy concerns [13,31]. Audio-based methods rely on recording sound patterns of workers' activities. However, this method faces challenges such as acoustic signal blockage by obstacles or interference from other sound signals [56].

The integration of these sensing technologies enables the acquisition of a substantial amount of objective activity-related data. Accordingly, previous studies have adopted machine learning algorithms to process these extensive datasets and achieve automatic and real-time activity recognition. Various machine learning algorithms such as support vector machine (SVM), decision tree (DT), k-nearest neighbor (KNN), linear discriminant analysis (LDA), and hidden Markov model (HMM), have been applied and refined for activity recognition of different objects on

construction sites [13]. In recent years, the advancement of deep learning has given rise to the development of algorithms such as autoencoders, convolutional neural network (CNN), and recurrent neural network (RNN)-based algorithms (e.g., long-short term memory (LSTM), gated recurrent unit (GRU)) for activity recognition tasks [16,31], including construction workers' activity classification problems [14,44]. These deep learning algorithms offer several important advantages that compensate for the limitations of conventional machine learning algorithms, including better performance on heterogeneous and large datasets, and automatic features learning through the training process [31,57], among others.

Despite important research progress, current research on sitting activity recognition of excavator operators or other construction equipment operators remains limited. Compared to workers who mainly perform manual handling activities, the limited overall activity space within the operating cockpit often obscures small amplitude of operator's body movement, presenting a significant obstacle for motion detection methods based on images or videos [13,16]. Many workers' activity recognition methods (e.g., computer vision-based and audio-based methods) rely on the workers' surrounding scenes [14], but the monotonous scene within the operating cockpit does not facilitate the effective segmentation of specific activities performed by the worker. Furthermore, the confined movement area of the operating cockpit results in minimal body movement during sitting activities, leading to a high degree of similarity in some sitting postures of construction equipment operators, such as sitting straight and leaning forward. This complexity presents challenges for accurately distinguishing between different activities using existing methods that rely on single sensing technology. To this end, advanced technologies suitable for sensing and identifying the sitting activities of excavator operators need to be further explored and developed.

2.2. Sitting activity sensing and recognition techniques

Sitting activities are closely related to people's performance at work and daily life. Previous research has underscored the practical significance of monitoring sitting activities, highlighting various aspects, including health risk assessment, production efficiency monitoring, and safety risk assessment [7,23,58-60]. For example, adopting prolonged awkward sitting postures, such as sagging or forward head postures, can lead to discomfort and pain in the cervical and lumbar spine [58], posing potential WMSDs risks [61]. Identifying and correcting these awkward sitting

postures can help alleviate corresponding health risks. From a safety perspective, analyzing sitting activities can provide insights into unsafe behaviors, as observed in road driving scenarios [62], such as driver distraction [63]. Activity recognition can provide valuable information for detecting and addressing such unsafe behaviors. Consequently, sitting activity sensing and recognition techniques have garnered extensive attention in various scenarios, including vehicle driving [28,60,64,65], office work [23-26], daily life [25,66], and healthcare [21,27].

In the construction equipment operating environment, where whole-body vibration is prevalent, operators often engage in prolonged work periods, which can lead to the adoption of poor operating postures or inappropriate actions. These factors contribute to the aforementioned risk issues. Several studies have highlighted that different sitting activities impact the level of exposure to mechanical equipment vibration, which is considered a common contributor to sitting discomfort and WMSDs [2,8,9]. Besides, sitting activity has been found to be associated with an individual's mental state. Prolonged awkward sitting posture (e.g., hunched back, forward sloping shoulders, curved spine, etc.) can induce mental fatigue and reduce cognitive performance [6,7,67-69]. Recognizing and correcting sitting activity can enhance intelligence and cognitive performance, alleviate anxiety and stress, and improve mental health. From an operational safety standpoint, prolonged operation and uncomfortable sitting postures have the potential to compromise attention and delay reaction times, directly impacting on-site operational productivity and impairing operational safety [1,6,70]. Consensus has been reached in studies indicating that continuous monitoring of worker activity can reduce accident rates and prevent injuries, falls, and WMSDs [71,72]. Additionally, with the construction industry undergoing industrialization and informatization changes, human-machine interaction on construction sites is becoming more prominent. The information provided by recognizing sitting activities plays a fundamental role in understanding various operating behaviors and machinery operation scenarios [11].

The existing methods for sensing and recognizing sitting activities align with the current state of research in general human activity recognition, including the recognition of construction worker activities. Commonly employed approaches in this domain include computer vision-based and kinematics-based methods [21,59,60,62,63,65,73]. However, most of these methods focus on distinguishing sitting activities from non-sitting activities, without accurately analyzing the specific types of activities performed while sitting. Recent studies have combined skeletal reconstruction [74], infrared array sensor [61], and radio frequency identification [75] to identify specific sitting

activities. Nevertheless, these approaches still face the challenges mentioned earlier.

Among these methods, sitting activity recognition based on interface pressure sensing technology has received much attention [23-28,76,77]. Interface pressure refers to the pressure exerted by the compression system over the skin's surface and is commonly used to assess a cushion's ability to manage pressure on the buttocks [78]. Interface pressure sensing technology offers several advantages that make it well-suited for collecting sitting posture-related data in construction equipment operation scenarios. First, pressure sensors provide a highly sensitive and quantitative means of measuring activity when direct observation or a limited number of inertial sensors is not feasible [79]. Second, pressure sensing units are minimally invasive and easy to deploy, making them a viable option for recognizing construction equipment operators' sitting activities. However, the complex characteristics of construction equipment operation scenarios present challenges when solely relying on this technology. As mentioned above, kinematic signal acquisition sensors are susceptible to the effects of vibration and irregular movements associated with construction equipment [80,81]. For instance, the collected interface pressure signal is inevitably superimposed with noise signals resulting from equipment activities. Considering the impact of these factors on activity recognition is crucial to enhance its performance. Furthermore, apart from recognizing static sitting postures, which have been the primary focus of existing research, it is crucial to consider the recognition of typical complex posture sequences during equipment operations. This necessitates further design and development in terms of indicator generation, recognition algorithm selection, and multi-sensor arrangement to effectively address this challenge.

3. Methods

3.1. Problem description and research framework

The recognition of excavator operators' sitting activities involves the collection and processing of posture-related data, which can be categorized into two aspects: static postures and dynamic compound actions [14]. Posture refers to the static configuration of the operator's body at specific moments, while action describes the dynamics of the consecutive body movements over a period of time. This paper systematically analyzes the details of sitting activities from these two perspectives. Based on the characteristics of the excavator operation scenario, a classification of excavator operators' sitting activities was constructed, as shown in Table 1. The classification includes seven static

sitting postures and nine compound sitting actions. Among them, sitting upright is a commonly observed posture and is considered an optimal position [82]. Leaning forward or backward can increase tension in the back or neck muscles, potentially leading to discomfort. Similarly, leaning left or right may cause muscle imbalances and contractures [83]. Crossing the left or right leg can result in sagittal imbalance, coronal imbalance, pelvic tilt, and spinal valgus angle [84]. The selection of sitting activities reflects the fundamental types of excavator operations.

Table 1 Predefined excavator operators' sitting activities.

Static sitting postures	**Compound sitting actions**
Sitting Upright (SU)	Move forward operation (MF)
Leaning Forward (LF)	Move left operation (ML)
Leaning Backward (LB)	Move right operation (MR)
Leaning Left (LL)	Swing operation
Leaning Right (LR)	Raising and lowering the boom (RL Boom)
Cross Left Leg (CLL)	Raising and lowering the arm (RL Arm)
Cross Right Leg (CRL)	Excavation operation
	Dumping operation
	Climbing operation

Fig. 1 presents the research framework proposed in this paper, which comprises five main components. First, an experiment was conducted at an actual excavator operating site to capture relevant data on the sitting activities outlined in Table 1. Second, the types of sensors and placement methods for data collection were designed. This section describes the data preprocessing process, involving metric quantification and sliding window techniques. Third, feature extraction was performed on the collected multi-sensor data, which is required for training machine learning algorithms. Three traditional machine learning algorithms and two RNN-based deep learning algorithms were employed. The final step involves training and evaluating the performance of the models. The performance of the trained models was assessed under various multi-sensor combination schemes. Further details of each component are provided below.

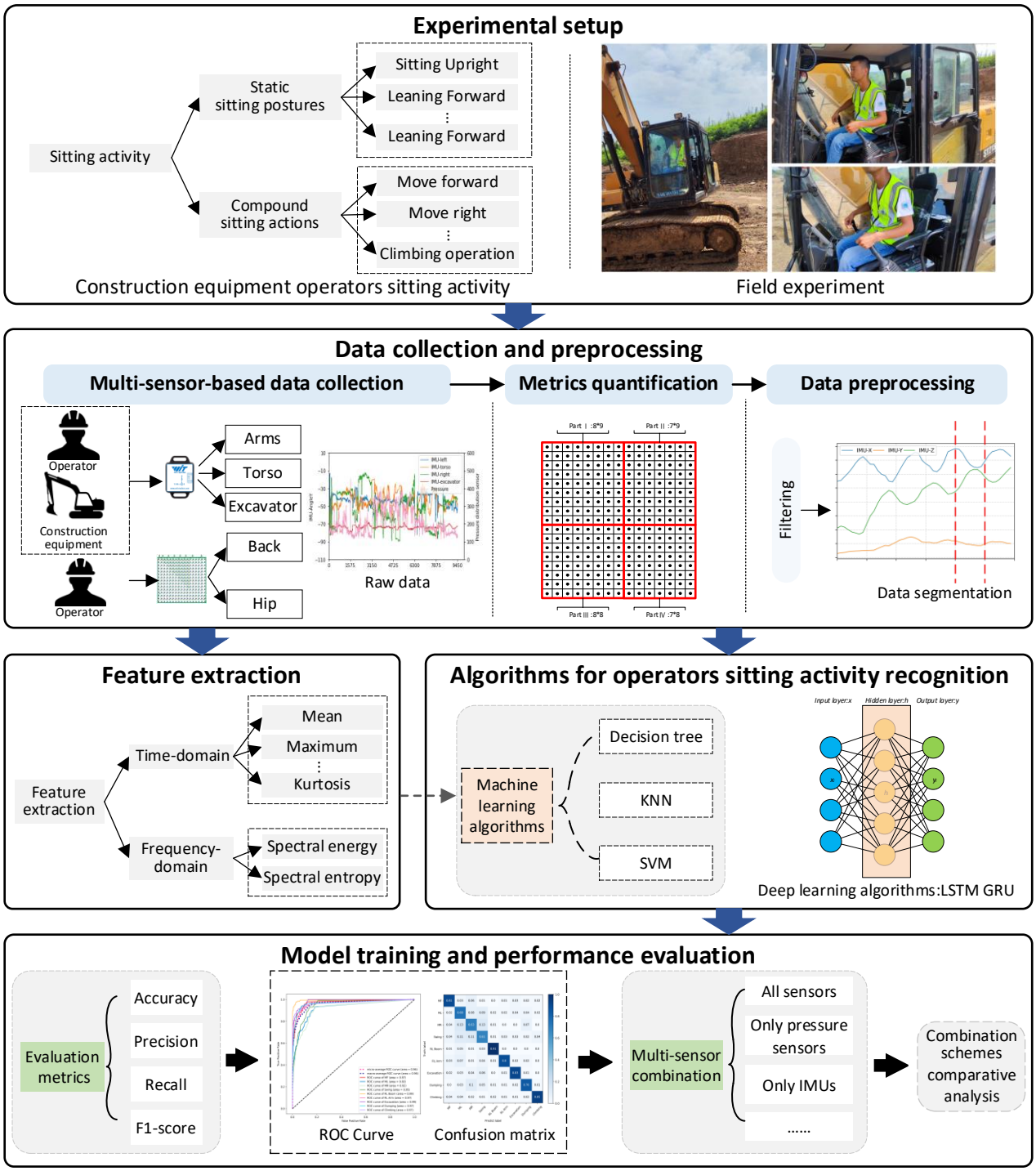

Fig. 1. Research framework.

3.2. Experimental setup

The experiments were conducted at an unobstructed highway construction site in Wuhan, China, providing an ideal setting for machinery operation. To comprehensively consider the diverse range of sitting postures and actions adopted by different operators, six highly skilled excavator operators with over five years of experience were recruited. The experimental data collection spanned for three sunny days to ensure optimal visibility and minimize task

disruption. Each day consisted of two rounds of data collection, comprising a pre-experiment training session and a formal experiment. Prior to each formal session, participants underwent a 30-minute training session to familiarize themselves with the experimental procedure and ensure a standardized approach to data collection. Following the experimental protocol requirements, two cushions with embedded flexible pressure sensor arrays were placed on the operator's seat, while four IMUs were positioned on their arms, torso, and equipment seat side wall, as illustrated in Fig. 2. It is noteworthy that conducting on-site data collection under completely uncontrolled conditions poses high safety risks. Furthermore, due to the short duration of certain sitting activities, there might be imbalances in the dataset, which could hinder the comprehensive capture of the temporal characteristics of diverse sitting activities. Therefore, to ensure the experiment safety and obtain sufficient data, the following experimental protocols were adopted.

Fig. 2. Construction site and field experiment data collection.

Experiment 1 (static sitting posture data collection): Participants were instructed to sit quietly in an excavator operating cabin and to perform each of the seven static sitting postures. Each posture was held for 90 seconds to ensure adequate data collection.

Experiment 2 (compound sitting actions data collection): Participants were required to sequentially perform nine common excavator operations. Each operation was executed continuously without interruption for approximately 90 seconds, culminating in a total experimental duration of approximately 810 seconds. This extended duration was

necessary to capture sufficient balanced datasets that accurately reflect the characteristics of the compound sitting actions.

During the data collection, each event was recorded using a video camera, and the pressure data and IMU data were synchronized. Based on the recorded video and each set of postures and actions, the time series of pressure data and IMU data were labeled by event type as the base facts.

3.3. Data collection and preprocessing

3.3.1. Multi-sensor-based data collection

Two types of sensors were utilized: the interface pressure sensor array and the nine-axis IMU, as shown in Fig. 3 (a). The Legact RPPS-255 pressure sensor array [85] was employed, featuring 255 pressure sensing units and a minimum detectable pressure of 20g. This sensor exhibits a rapid response time (<10us) and supports the series connection of multiple sensors, making it highly adaptable for the data collection requirements. The IMU developed by WitMotion [86] integrates digital angle, gyroscope, accelerometer, and compass sensors, coupled with a high-performance microprocessor. These features enable the IMU to effectively capture subtle variations in arms and torso amplitudes across different operators' sitting activities.

Two interface pressure sensor arrays were used to capture the temporal changes in pressure distribution between the operator and the seat. Each array consists of a pressure sensing module, a signal acquisition module, and a digital signal processing module. Fig. 3 (b) illustrates the workflow of the sensor arrays. The pressure sensor array comprises 255 sensing units with a dense distribution of 15×17 units, all possessing identical specifications. Each sensing unit is placed at a 30×30 mm^2 interval, with a diameter of 14 mm and a gap of 16 mm, ensuring accurate capture of pressure electrical signal. The sensor array was calibrated to collect pressure data from 255 units at a frequency of 50 Hz. To ensure cushion comfort and minimize potential invasiveness on the operator's body, modifications were made to the pressure sensor array by utilizing different materials, as depicted in Fig. 3 (e). The sensor arrays were mounted on the excavator's seat cushion and backrest, as shown in Fig. 3 (d), with the blue region indicating the sensor locations. This modification aimed to strike a balance between comfort and avoiding damage caused by excessive sensor bending.

Furthermore, four nine-axis IMUs were employed to record the changes in posture angles of the operator's arms, torso, and the excavator, as depicted in Fig. 3 (c). Specifically, three IMUs were placed on the operator's torso and the left and right arms. Additionally, an IMU was installed on the side wall of the seat to record the excavator's movements without intruding on the operator. The primary purpose of collecting IMU data is to supplementarily capture the operator's sitting postures and movements across various operational tasks, as well as the simultaneous vibrations and movements of the excavator. The IMU outputs acceleration, angular velocity, angle, and magnetic field data along the three axes of the operator's motion. The data was collected at a frequency of 50 Hz, and a Kalman filter was automatically applied to reduce measurement noise, enhance accuracy, and enable real-time motion recording [87].

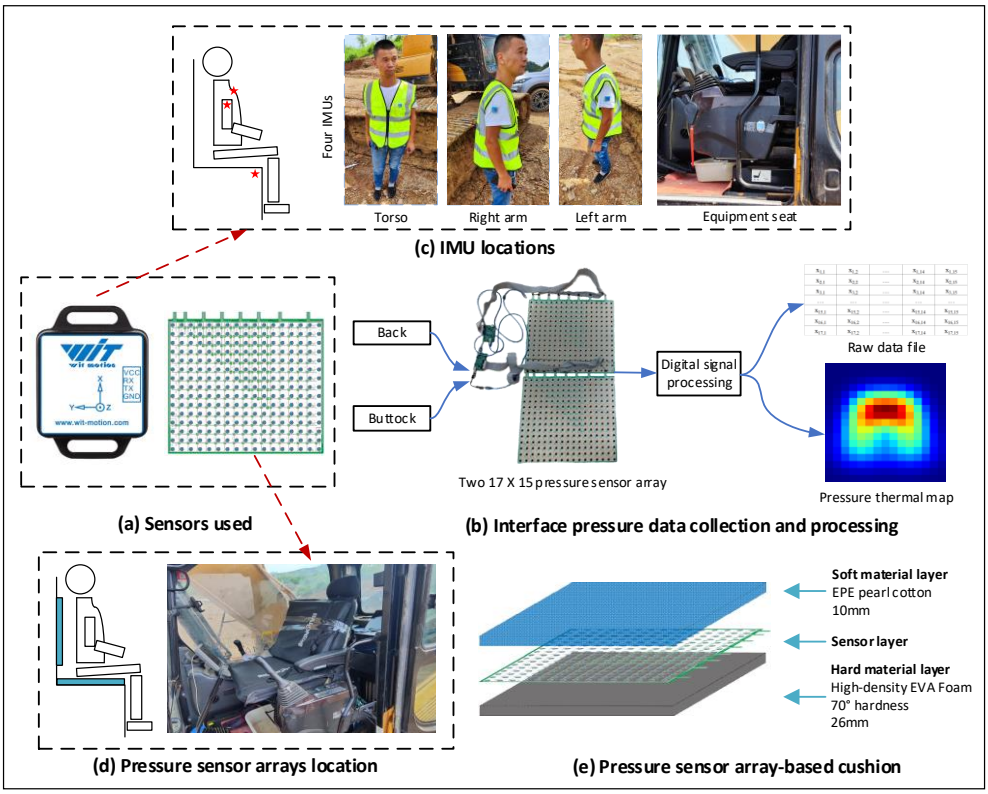

Fig. 3. The proposed multi-sensor system and experimental placement.

Preliminary analysis of the collected raw data from multiple sensors can reveal the complex signal characteristics of the construction equipment operating environment. Fig. 4 illustrates the fluctuation curves of the IMUs and pressure sensors over time. The Y-axis angle recorded by a single IMU and the average pressure of the region of interest (ROI) in the upper left corner of the seat cushion (the detailed ROIs are described in detail in Section 3.3.2) were selected as representative samples from the original datasets. Fig. 4 (a) clearly illustrates distinct data changes

at the transition between different activities. Moreover, Fig. 4 (a-d) indicate that the IMUs attached to the operator's body exhibit the similar fluctuation trend to the IMU installed on the equipment. This suggests that equipment activity introduces certain interference with the quality of the operators' sitting activity data.

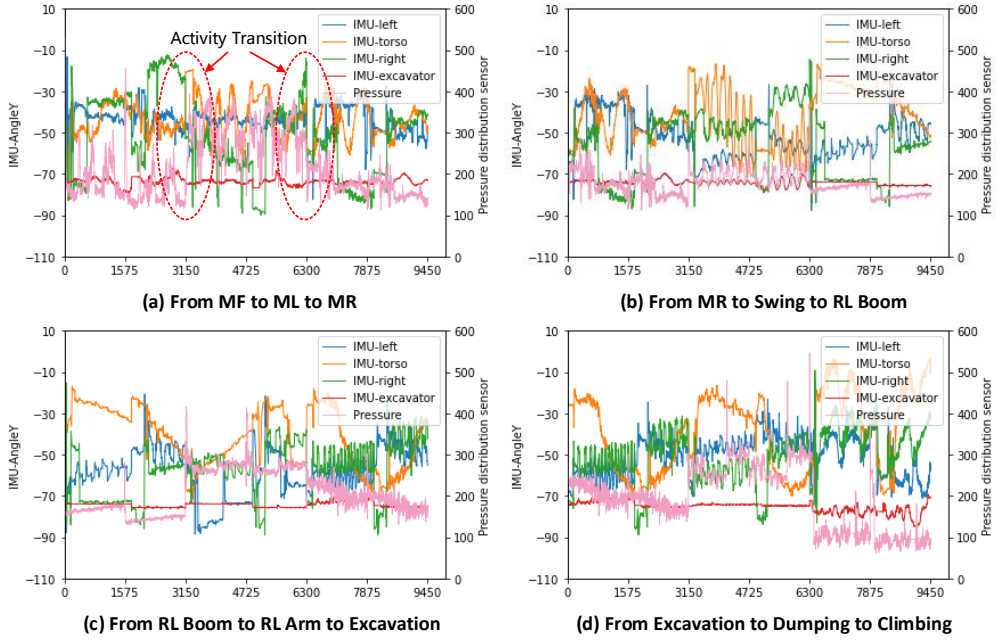

Fig. 4. Multi-sensor data of excavator operator's sitting activities.

3.3.2. Metrics quantification

The pressure sensor array captures only the interface pressure value from each unit, which provides limited information. To enhance the accuracy of model training and obtain more meaningful features, the raw pressure data was utilized to calculate additional pressure metrics. This approach aims to derive physically meaningful features that exhibit a high correlation within the pressure domain. To achieve this, six main ROIs were defined in the two sensor arrays based on the delineation of body areas according to the discomfort scale for body parts and the interface regions between the human body and the seat [28,88], as illustrated in Fig. 5. The utilization of pre-defined ROIs to calculate corresponding interface pressure metrics has been employed in prior studies [26,28,89]. A coordinate system was established on each of the two sensor arrays, with the upper left sensing unit as the origin, to quantify the metrics. Each sensor unit was assigned an integer coordinate. In total, 40 quantitative metrics were obtained (Table 2), including: (1) 12 parameters indicating average contact areas and ratios [28]; (2) 12 parameters representing average contact pressures and ratios; (3) 12 parameters describing average peak contact pressures and ratios; (4) 4 parameters calculating the location of the center of gravity of the pressure cushion. On this basis, the above-mentioned metrics

can be calculated as follows.

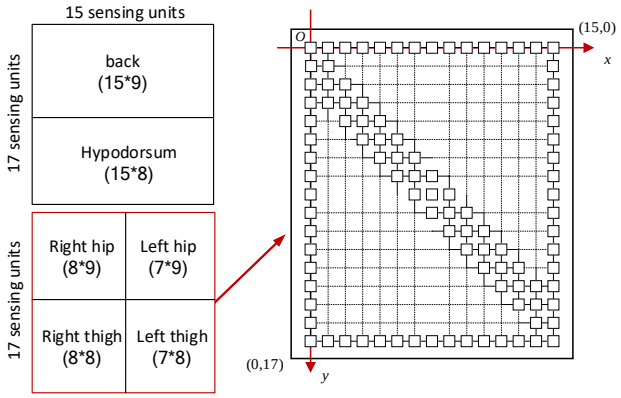

Fig. 5. Segmentation of ROIs in pressure sensor array and the coordinate system.

(1) Contact area:

$$Contact\ area_{ROI\ i} = Sum(\sum_{x,y} p(x,y,t) > 0) \tag{1}$$

where $p(x,y,t)$ represents the pressure value recorded by each sensor at each moment. $ROI\ i$ represents the i-th region of interest. As illustrated in Fig. 5, a total of 6 ROIs are identified.

(2) Contact area ratio:

$$Contact\ area\ ratio_{ROI\ i} = \frac{Contact\ area_{ROI\ i}}{\sum_i Contact\ area_{ROI\ i}}. \tag{2}$$

(3) Average pressure:

$$Average\ pressure_{ROI\ i}(t) = \frac{\sum_{x,y} p'(x,y,t)}{Contact\ area_{ROI\ i}} \tag{3}$$

where only pressure values greater than 0 were included in the statistics.

(4) Average pressure ratio:

$$Average\ pressure\ ratio_{ROI\ i} = \frac{Average\ pressure_{ROI\ i}}{\sum_i Average\ pressure_{ROI\ i}}. \tag{4}$$

(5) Average peak pressure:

$$Average\ peak\ pressure_{ROI\ i} = Max(p(x,y,t)_{ROI\ i}). \tag{5}$$

where this indicator records the maximum value recorded by the pressure sensor in each ROI per unit time.

(6) Average peak pressure ratio:

$$Average\ peak\ pressure\ ratio_{ROI\ i} = \frac{Average\ peak\ pressure_{ROI\ i}}{\sum_i Average\ peak\ pressure_{ROI\ i}}. \tag{6}$$

(7) Center of Pressure (COP):

COP is a common metric in analyzing the postural sway and is often used to indirectly assess the level of discomfort

and fatigue in a sitting position [90]. In this paper, the COPs were calculated for both pressure arrays, which are quantified as:

$$COP_x = \frac{\sum p(x,y,t)*x_i}{\sum p(x,y,t)};\ COP_y = \frac{\sum p(x,y,t)*y_i}{\sum p(x,y,t)} \quad (7)$$

where in the process of index calculation, the coordinates of each sensor are shown in Fig. 5 (with the sensor in the upper left corner as the origin).

Table 2 Interface pressure metrics for excavator operators' sitting activity recognition.

Metric categories	Metrics	Description	Reference
Average contact area	$Contact\ area_{ROI\ i}$	Contact area per subarea (in practice, expressed as the number of sensors with pressure values greater than 0 in a single subarea).	[26,28,91]
Average contact area ratio	$Contact\ area\ ratio_{ROI\ i}$	Ratio of average contact pressure per sub-area to total contact area ($\sum_i Contact\ area_{ROI\ i}$).	[28]
Average pressure	$Average\ pressure_{ROI\ i}$	The average pressure of each ROI over an interval of 8 frames.	[26,28,29,91]
Average pressure ratio	$Average\ pressure\ ratio_{ROI\ i}$	Ratio of average pressure per sub-area to total pressure ($\sum_i Average\ pressure_{ROI\ i}$).	[28]
Average peak pressure	$Average\ peak\ pressure_{ROI\ i}$	The highest pressure appearing in each ROI during the time interval of 8 frames.	[26,28,29,91]
Average peak pressure ratio	$Average\ peak\ pressure\ ratio_{ROI\ i}$	Ratio of the highest pressure in each ROI in 8 frames to the sum of the highest pressure values in each region ($\sum_i Average\ peak\ pressure_{ROI\ i}$).	[28]
Center of pressure (COP)	$COP_x;\ COP_y$	The location of the center of gravity of the pressure cushion.	[76]

3.3.3. Data preprocessing

To address the small amount of missing data in the collected dataset, the linear interpolation method was employed to fill in the missing values within the time series. Additionally, a few instances of abnormal pressure values exceeding the maximum range of the pressure sensor were detected in the raw data, and these outliers were removed from the dataset. In the data segmentation process, real-time updates were implemented using sliding windows that encompass adjacent samples. As new data was added to these windows, the oldest samples were discarded. This approach ensures that the window perpetually refreshes its contents, thereby enhancing the model's updating efficiency and adaptability [92]. Determining the optimal window size is critical to using the sliding window approach [93]. Previous studies have used a range of window sizes from 0.25 to 6.7s depending on the types of activities to be recognized [94]. In this paper, the data acquisition was conducted at a sampling frequency of 50 Hz, with each frame lasting 0.02s. In the

previous metrics quantification process, a time interval of 8 frames was used, resulting in the sliding window being divided multiple times by 0.16s each. The results confirm that employing a sliding window of 5.12s, which yields a total of 256 sets of data per window, leads to a highly accurate model. The overlap of consecutive windows was performed to prevent missing relevant data. Drawing on previous similar studies [44,95], an overlap of 50% in the length of adjacent data segments was employed.

3.4. Feature extraction

Machine learning efficacy hinges on quality input information. Feature extraction plays a pivotal role in isolating relevant information from raw data to construct models [96]. It compresses input data dimensionality, bolstering model performance by discarding extraneous noise and data [97]. This paper extracted features from time and frequency domains. For the pressure-related data, time domain features including mean, maximum, minimum, extreme deviation, variance, standard deviation, and kurtosis were used. The time-domain features were converted to the frequency domain using the self-contained fast Fourier transform (FFT) function [98,99]. Two frequency domain features, namely spectral energy and entropy, were extracted [99]. Spectral energy provides insights into the distribution of signal energy across different frequencies, while spectral entropy measures the irregularity of the signal by calculating the normalized information entropy of the discrete FFT component amplitudes [99]. Regarding the IMU-related data, acceleration, angular velocity, and angle data were obtained within a certain sliding window. The vector magnitude $\sqrt{x^2+y^2+z^2}$ was combined and extracted the features of mean, maximum, minimum, extreme deviation, variance, standard deviation, kurtosis, spectral energy, and entropy for the corresponding data of vector magnitude, x-axis, y-axis, and z-axis within the given window, respectively [100].

3.5. Algorithms for operators' sitting activity recognition

Machine learning algorithms have been widely used for human activity recognition [77,101]. Traditional approaches require pre-model training feature extraction from raw data, heavily depending on domain expertise [102]. These features, especially time and frequency-related, are essentially linear, contrasting with the nonlinearity in real-world human behavior recognition, often resulting in inaccuracies [103]. Conversely, deep learning algorithms

automatically derive translational invariant and robust features from sensor data, diminishing the need for manual extraction and selection [31]. They incorporate both feature extraction and activity classification within the model construction process [97,104], making them increasingly prevalent in human activity recognition [105]. This paper employed both machine learning and deep learning algorithms for recognizing the sitting activities of excavator operators, with specific algorithms elaborated in subsequent sections.

3.5.1. Machine learning algorithms

The process of traditional machine learning is shown in Fig. 6. Previous studies [77,93,106] have employed various supervised machine learning algorithms for human activity recognition. In line with this, three widely used machine learning algorithms were selected in this paper: DT, KNN, and SVM.

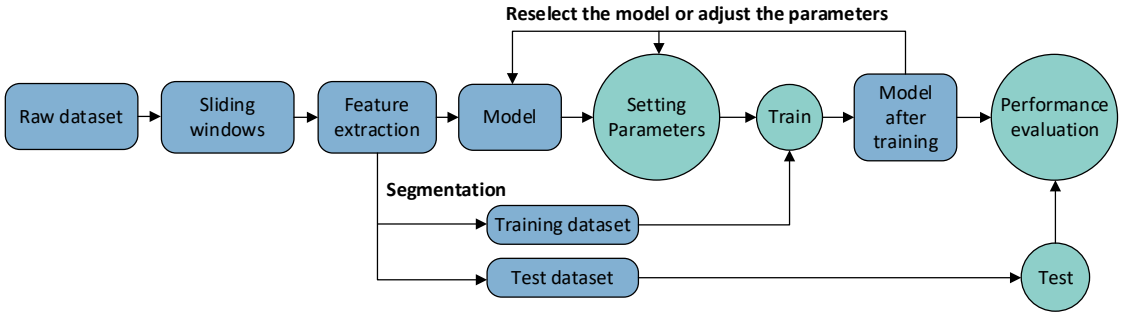

Fig. 6. Basic flow chart of statistical machine learning.

(1) DT

DT is a foundational classifier in supervised machine learning [107], employing tree structures for decision-making. In this paper, entropy is utilized to assess split quality, effectively mitigating the impact of dominant classes on overall purity.

(2) KNN

KNN stands out for its simplicity, directness, and adaptable implementation [108]. It diverges from typical classifiers by eschewing a learning phase, instead retaining the entire dataset for a direct classification approach. KNN assigns categories to new data points based on their proximity (distance) to known samples in the training set [109], with Euclidean distance as the metric in this paper.

(3) SVM

SVM is esteemed for its efficient learning with minimal parameters, resilience against model deviations, and computational prowess [110]. Its kernel function transforms the input from lower to higher-dimensional spaces,

enriching the feature representation [111]. This paper employs the Gaussian radial basis function as the kernel, selected for its proven superior learning rates in prior research [70,106].

3.5.2. Deep learning algorithms

RNN is a type of neural network specifically designed for processing sequence data. An RNN contains input layers, hidden layers, and output layers. The activation functions control the output, and the layers are interconnected through weighted connections [112]. Fig. 7 (a) illustrates the standard structure diagram of an RNN. Each arrow in the diagram represents a transformation, indicating the connections with corresponding weighted values. The left side is the folded look, and the right side is the unfolded look. x denotes the input, h represents the hidden layer element, o signifies the output, L is the loss function, and y is the label of the training set. The t in the upper right corner of these elements represents the state of the t moment, where it should be noted that the performance of the hidden unit h at the t moment is not only determined by the input at the t moment, but also influenced by the moment before the t moment. The weights V, W, and U are connected based on their respective types. In the following parts, two RNN-based deep learning algorithms are proposed for classifying different types of sitting activities.

(1) LSTM

LSTM is a specialized type of recurrent neural network capable of analyzing time series. It effectively overcomes the long-term dependency issues commonly encountered in general RNNs, ensuring that valuable information from the past is retained. Furthermore, LSTM addresses the issue of gradient disappearance or explosion in RNNs [113].

The core of LSTM is the cell state, represented by horizontal lines running through the cell. It is represented in Fig. 7 (b) by C_{t-1} to C_t. The LSTM network modifies or adds information about the state of cells through a gate structure, namely the forget gate (f_t), the input gate (i_t), and the output gate (o_t) [113]. The forget gate (f_t) determines which information in C_{t-1} needs to be retained or discarded by considering h_{t-1} andx_t. The input gate (i_t) decides which new information should be incorporated into the cell structure. The output obtained from the forget gate and the input gate generates a new cell C_t. The output gate (o_t) specifies which information in the cell state is to be used as the final output of the LSTM. The gate structure, cell state (C_t) and hidden state (h_t) of the cell are calculated as follows [114]:

$$f_t = \sigma(W_f . [h_{t-1}, x_t] + b_f) f_t \quad (8)$$

$$i_t = \sigma(W_i \cdot [\, h_{t-1}, x_t] + b_i)\, i_t \tag{9}$$

$$\hat{\mathrm{C}}_t = \tanh(W_c \,.\, [\, h_{t-1}, x_t] + b_c) \tag{10}$$

$$C_t = f_t \cdot C_{t-1} + \, i_t \cdot \hat{\mathrm{C}}_t \tag{11}$$

$$o_t = \sigma(W_o \,.\, [\, h_{t-1}, x_t] + b_o) o_t \tag{12}$$

$$h_t = o_t \cdot tanh(C_t)\, h_t \tag{13}$$

where σ is an activation function, and the softmax function is generally used. W_f, W_i and W_o are the weights for the forget, input, and output gates at time step t, respectively. W_c is the weight for the candidate layer. x_t represents the input at the current time step t. h_t and h_{t-1} are the respective outputs of the cell at the current time step t and previous time step $t-1$. C_t and C_{t-1} are the cell states at time steps t and $t-1$, respectively.

(2) GRU

GRU is an enhanced variant of the standard RNN that achieves comparable performance with fewer parameters and a more straightforward structure than LSTM, making it easier to train and greatly improving training efficiency [114,115]. Similar to LSTM, GRU is designed to reset or update its memory adaptively [44]. The main distinction from LSTM is that GRU employs only two gates, called reset gate (r_t) and update gate (z_t). The former corresponds to the input gate and forget gate of LSTM, and the latter is used to hide the state.

The GRU cell architecture is shown in Fig. 7 (c). First, the state of the two gates was obtained from the last transmitted state h_{t-1} and the input x_t of the current node, where r_t controls the reset gate and z_t controls the update gate. After getting the gating signal, reset gating was used to get the reset data h_{t-1}', h_{t-1}' is then spliced with input x_t, and the data is scaled between -1 and 1 by the tanh activation function to obtain $\hat{\mathrm{h}}_t$. Finally, the network computes the hidden state h_t, which is a vector that carries information for the current unit and passes it to the network [44]. The calculation process is shown in the following equations.

$$z_t = \sigma(W_z \,.\, [\, h_{t-1}, x_t] + b_z) z_t \tag{14}$$

$$r_t = \sigma(W_r \,.\, [\, h_{t-1}, x_t] + b_r) r_t \tag{15}$$

$$\hat{\mathrm{h}}_{\,t} = \, tanh(W \cdot [r_t \, \times \, h_{t-1}, x_t] + \, b_h \,) \tag{16}$$

$$h_t \, = (1 - z_t) \times \, h_{t-1} \, + \, z_t \, \times \hat{\mathrm{h}}_t. \tag{17}$$

Here, σ denotes the sigmoid function that converts the data to a value in the range of 0 to 1 to act as a gating

signal. z_t and r_t are the output of the update and reset gates. W_z and W_r are the weights for the update and reset gates. b_z and b_r are the biases for the update and reset gates. h_t and h_{t-1} are the respective outputs of the cell at the current time step t and previous time step $t-1$. x_t is the input at the current time step t.

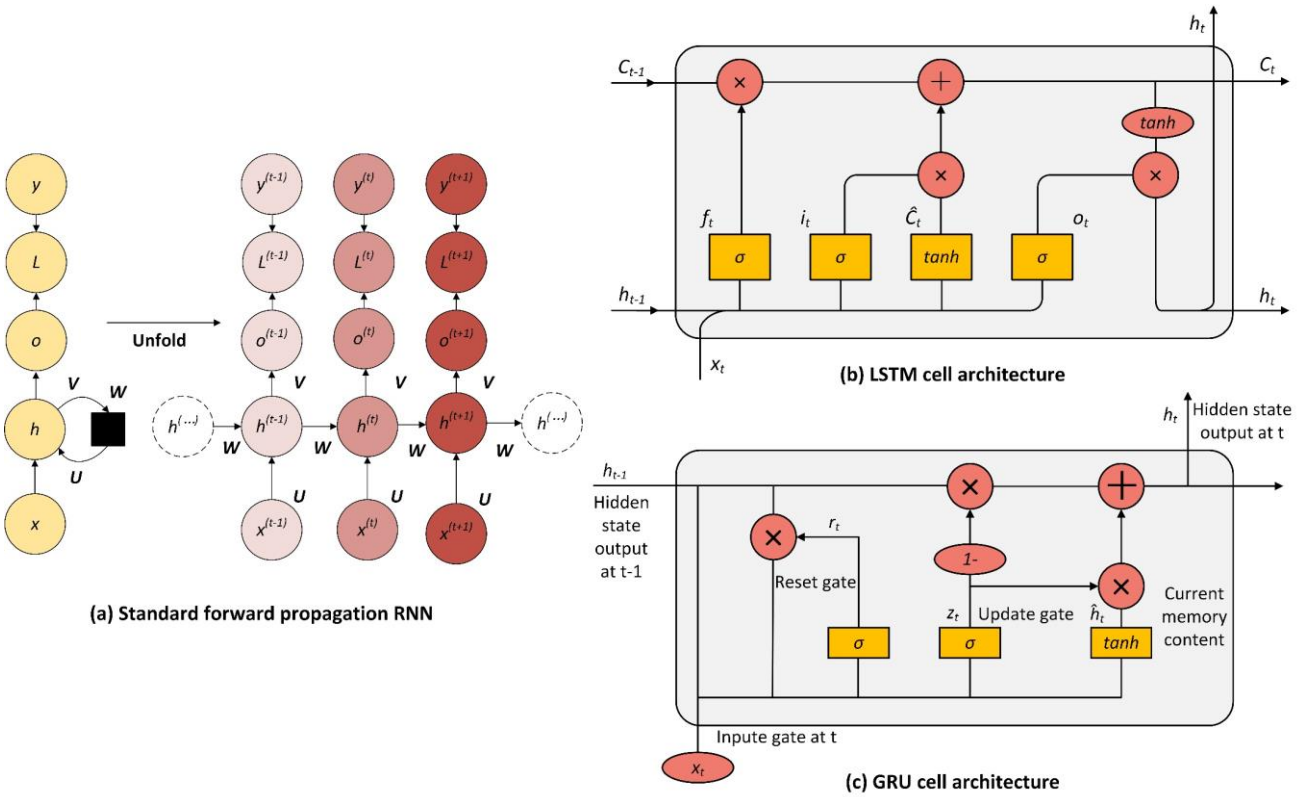

Fig. 7. Architectures of recurrent neural networks: Standard RNN, LSTM, and GRU.

3.6. Model training and performance evaluation

In the model training phase, LSTM and GRU were trained with pre-processed, non-feature-extracted multi-sensor data, contrasting with supervised machine learning algorithms (i.e., DT, KNN, and SVM) that utilized feature-extracted datasets. The paper employed the leave-one-subject-out (LOSO) cross-validation approach, designating a single subject's dataset as the test set while amalgamating data from all other subjects for training. This approach maximizes data utilization from each participant and significantly mitigates subject bias due to individual variability, a practice prevalently endorsed in worker activity recognition research [70,98]. The deep learning models were constructed using a sequential framework, each initiated with three homogeneous recurrent layers of corresponding types (LSTM and GRU), equipped with 512 hidden units per layer. Previous research indicated that similar architectures can achieve the highest classification accuracy [116]. To mitigate potential overfitting issues, a dropout

layer with a rate set to 0.2 was integrated into the model, which is a commonly used method for random regularization [117]. The output layer of the model is a dense layer, with the number of neural units corresponding to the number of categories in the classification task. Mean squared error was utilized as the cost function to measure model accuracy [44]. The initial learning rate was set at 0.001 and the ReduceLROnPlateau callback function was employed during training to dynamically adjust the learning rate, thereby optimizing model performance. Other hyperparameters were tuned to ascertain the optimal values that provide the highest accuracy while minimizing training time. The results indicated that optimal accuracy was achieved with epochs, batch size, and optimizer values set to 50, 32, and RMSProp, respectively. Experiments were conducted using Python 3.6 on an Intel Xeon Processor (Skylake, IBRS), with 32GB RAM, a 64-bit Windows 10 operating system, and a V100-32G GPU.

The performance of machine learning and deep learning algorithms was evaluated using accuracy, precision, recall, and F1-score (Eq. 18-21). Accuracy provides an overall assessment of the model's performance across all classes. Precision measures the ability of the model to avoid incorrectly labeling negative instances as positive. Recall focuses on the model's capability to correctly identify all positive instances. F1-score provides a balanced measure of the model's performance by considering both precision and recall. Additionally, individual class performance is analyzed through confusion matrices, while receiver operating characteristic (ROC) curves for each category provide a quantitative assessment of classifier quality through the calculation of the area under the curve.

$$Accuracy = \frac{TP + TN}{TP + TN + FP + FN} \tag{18}$$

$$Precision = \frac{TP}{TP + FP} \tag{19}$$

$$Recall = \frac{TP}{TP + FN} \tag{20}$$

$$F1 - score = 2 \times \frac{Precision \times Recall}{Precision + Recall}. \tag{21}$$

Where true positive (TP) represents the number of positive instances correctly classified as positive, true negative (TN) represents the number of negative instances correctly classified as negative, false positive (FP) represents the number of negative instances incorrectly classified as positive, and false negative (FN) represents the number of positive instances incorrectly classified as negative.

4. Results

4.1. Effectiveness of the proposed recognition algorithms under multi-sensor data

In the context of operators' sitting activities, the combination of multiple sensors is categorized into six groups, as illustrated in Table 3. The excavator's low-amplitude uniform vibrations during the collection of static sitting posture data have limited impact on the pressure sensor. As a result, the algorithm performance for the 1st and 6th multi-sensor combination schemes in static sitting posture recognition is comparable. Therefore, the 6th combination scheme is not considered for static sitting posture recognition. Consequently, a dataset comprising 73,500 instances of static sitting postures and 94,500 instances of compound sitting actions was collected for this paper. The analysis primarily aimed to compare the performance of the multi-sensor combinations using different algorithms.

Table 3 Multi-sensor combination schemes.

#	Combination schemes
1	Only use pressure sensors
2	Only use IMUs
3	Fusion of pressure sensors and all IMUs
4	Fusion of pressure sensors and the IMU at the torso
5	Fusion of pressure sensors and the IMUs at the arms
6	Fusion of pressure sensors and the IMU at excavator seat side wall

(1) Static sitting posture recognition

The results reveal that the overall accuracy of static sitting posture recognition among different multi-sensor combinations ranges from 76.14% to 98.50%. This can be attributed to the relatively stable nature of static sitting postures over time, allowing for the acquisition of a relatively stable and clean dataset under ideal conditions. Traditional machine learning algorithms often achieve high classification accuracy by extracting features in the time domain. Among all the algorithms, SVM (95.69% accuracy), LSTM (97.90% accuracy), and GRU (98.50% accuracy) exhibit high classification accuracy when using the multi-sensor combination scheme where all sensors are utilized (scheme #3). In this paper, the performance of SVM, LSTM, and GRU under scheme #3 is further evaluated through the use of confusion matrices and ROC curves.

Table 4 Recognition performance of static sitting postures under five algorithms with different multi-sensor combinations.

Algorithm	Scheme	Classification performance (%)			
		Accuracy	Precision	Recall	F1-Score
DT	1	0.8743	0.8751	0.8743	0.8744
	2	0.9307	0.9310	0.9308	0.9307

	3	0.9434	0.9435	0.9435	0.9434
	4	0.9426	0.9427	0.9427	0.9425
	5	0.9428	0.9430	0.9428	0.9428
SVM	1	0.7614	0.7722	0.7603	0.7591
	2	0.9226	0.9235	0.9230	0.9227
	3	0.9569	0.9571	0.9571	0.9569
	4	0.9485	0.9478	0.9477	0.9472
	5	0.9550	0.9551	0.9550	0.9548
KNN	1	0.7778	0.7802	0.7780	0.7781
	2	0.9265	0.9264	0.9271	0.9263
	3	0.9480	0.9483	0.9481	0.9480
	4	0.9411	0.9417	0.9410	0.9410
	5	0.9458	0.9455	0.9449	0.9450
LSTM	1	0.9339	0.9334	0.9336	0.9333
	2	0.9265	0.9269	0.9263	0.9263
	3	0.9790	0.9886	0.9788	0.9786
	4	0.9554	0.9550	0.9554	0.9550
	5	0.9502	0.9593	0.9507	0.9596
GRU	1	0.9446	0.9447	0.9444	0.9444
	2	0.9350	0.9353	0.9348	0.9348
	3	0.9850	0.9849	0.9849	0.9848
	4	0.9788	0.9787	0.9789	0.9787
	5	0.9800	0.9802	0.9800	0.9800

The confusion matrix (Fig. 8 (a)) reveals the high classification accuracy of distinct static sitting postures by three algorithms. Misclassification between LR and CLL is noted, likely influenced by asymmetric pressure distribution. The SVM algorithm excels, with accuracies predominantly above 90%, though it confounds LF and LB, possibly owing to data collection adjacency and the operator's incomplete leaning. Conversely, GRU and LSTM surpass 90% accuracy across all posture types, benefiting from deep learning's intrinsic automatic feature extraction, which outperforms manual methods.

The ROC curve, depicted in Fig. 8 (a), demonstrates the interplay between true positive rate (TPR) and false positive rate (FPR) across thresholds. The area under the ROC curve (AUC) serves as a robust classifier comparison metric, unaffected by case proportion. Most AUC values exceed 0.98, underscoring classifier efficacy. Notably, deep learning algorithms exhibit superior AUC values compared to SVM, affirming their enhanced performance in static sitting posture classification.

In Fig. 9 (a), the GRU model's accuracy and loss curves under scheme #3 are depicted. As training epochs increase, there is a notable enhancement in accuracy across training and validation sets, while loss consistently diminishes. The convergence of these indicators at the 45th epoch demonstrates that the GRU model has been effectively trained,

achieving this without overfitting the static sitting posture data.

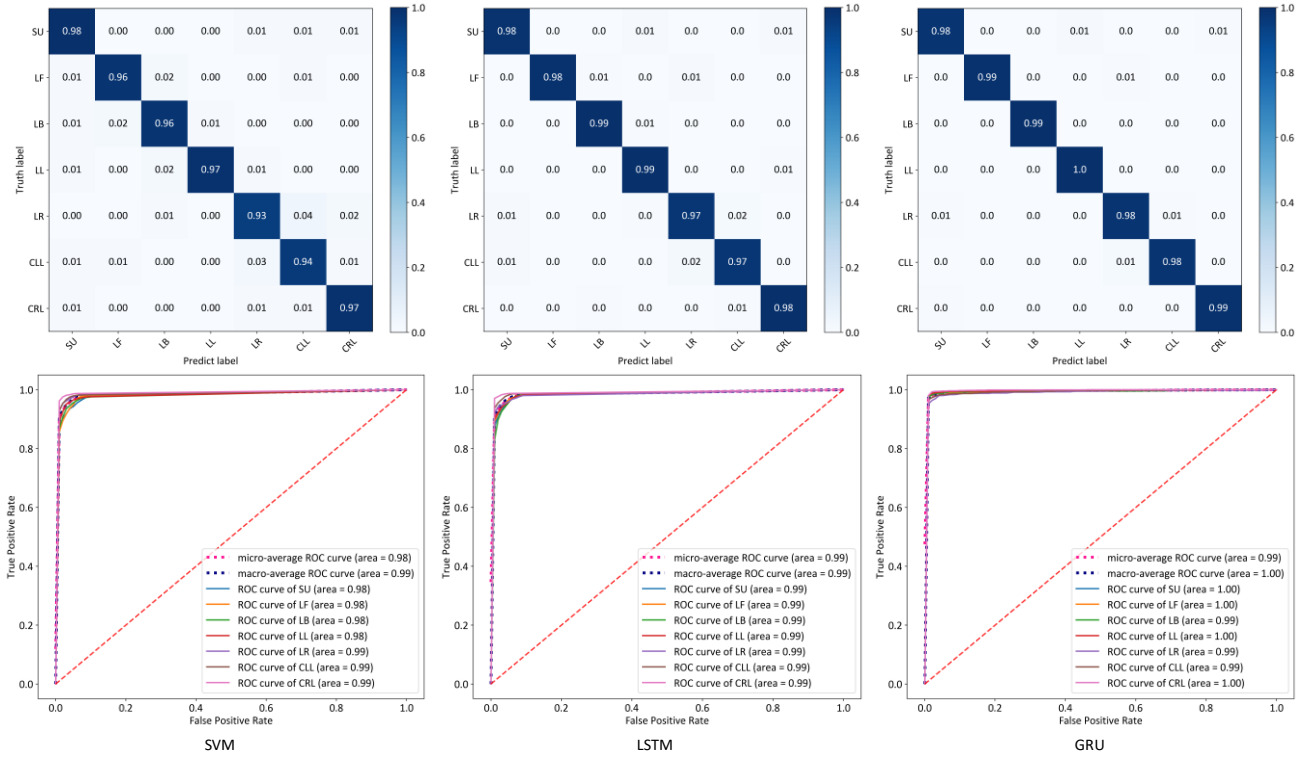

(a) Confusion matrix and ROC curve for static sitting postures (scheme #3)

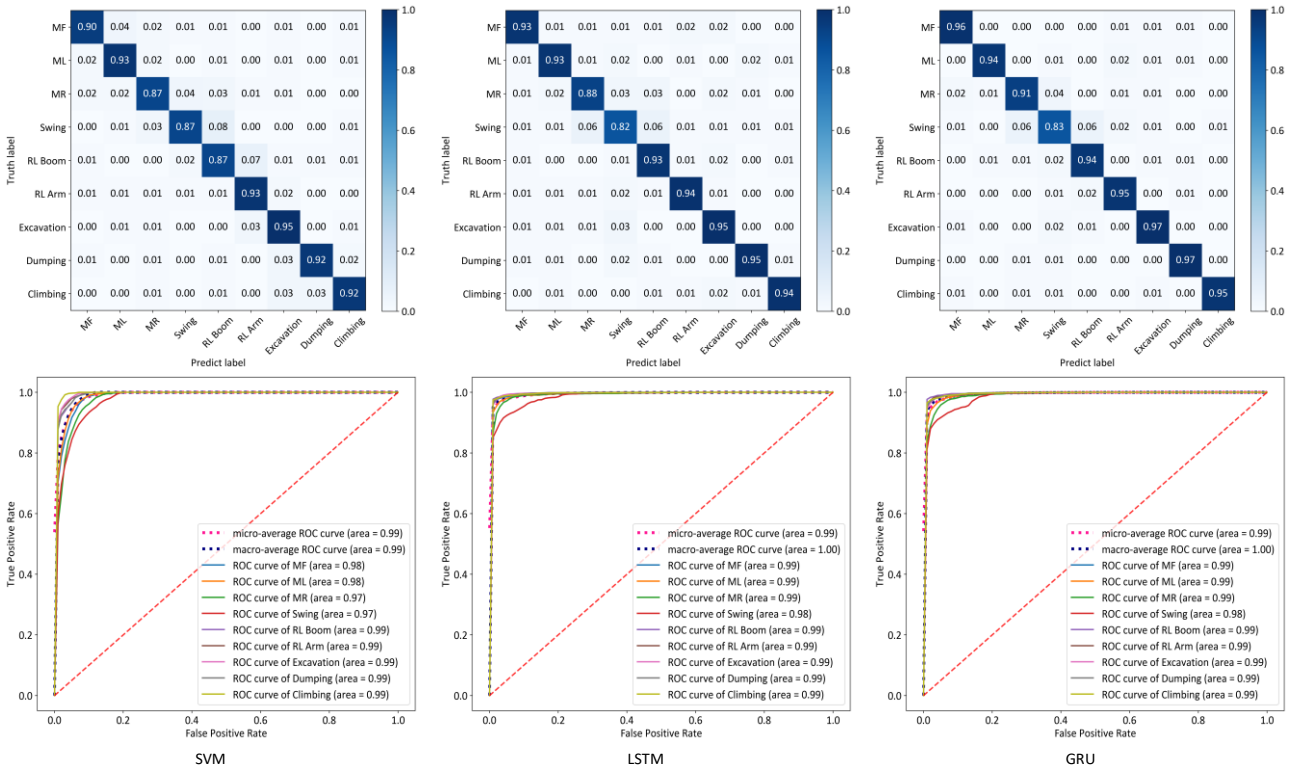

(b) Confusion matrix and ROC curve for compound sitting actions (scheme #3)

Fig. 8. Confusion matrix and ROC curve.

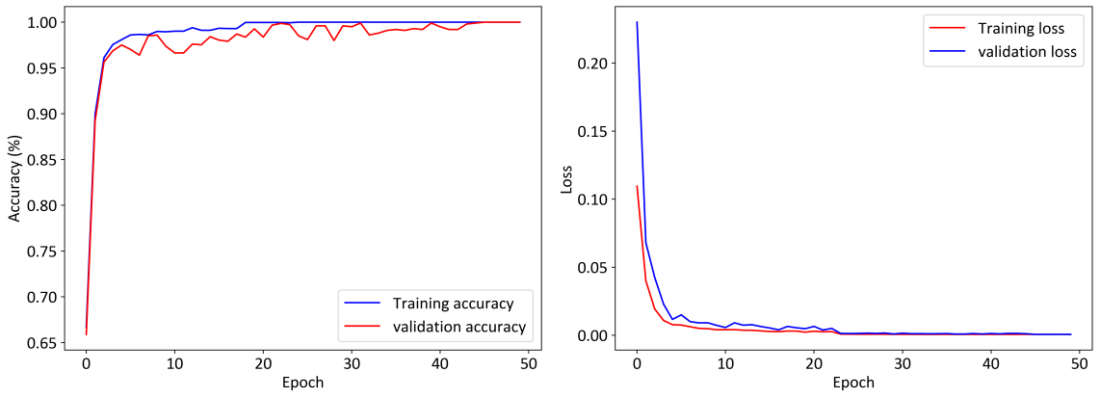

(a) Iterative accuracy and loss curve of GRU model in static sitting postures

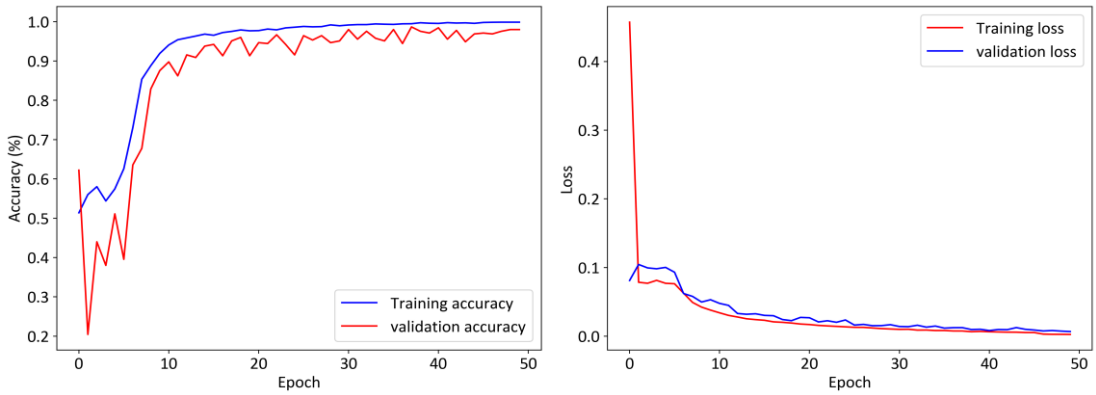

(b) Iterative accuracy and loss curve of GRU model in compound sitting actions

Fig. 9. Iterative accuracy and loss curve of GRU model under scheme #3.

(2) Compound sitting action recognition

Regarding the recognition of compound sitting actions, the results differ. Table 5 demonstrates that GRU (94.25% accuracy) consistently outperforms other algorithms in terms of classification accuracy for compound sitting actions in different combination schemes. This is because compound sitting actions are considered a fusion of various arm postures and static sitting postures. GRU models are distinguished by their unique model characteristics and exhibit significant advantages in handling time series data. Among traditional machine learning algorithms, SVM (93.86% accuracy) performs relatively better. In the following sections, the performance of SVM, LSTM, and GRU was further evaluated using confusion matrices and ROC curves, utilizing a scheme where all sensors are employed.

Table 5 Recognition performance of compound sitting actions under five algorithms with different multi-sensor combinations.

Algorithm	Scheme	Classification performance (%)			
		Accuracy	Precision	Recall	F1-Score
DT	1	0.7952	0.7949	0.7980	0.7953
	2	0.7575	0.7649	0.7573	0.7577
	3	0.9028	0.9024	0.9024	0.9018
	4	0.8836	0.8841	0.8847	0.8836
	5	0.8869	0.8875	0.8875	0.8868
	6	0.8611	0.8607	0.8607	0.8601
SVM	1	0.8048	0.8125	0.8062	0.8028

	2	0.7766	0.7743	0.7788	0.7724
	3	0.9386	0.9373	0.9373	0.9371
	4	0.9262	0.9243	0.9238	0.9239
	5	0.9346	0.9340	0.9342	0.9340
	6	0.8987	0.8974	0.8974	0.8972
KNN	1	0.7140	0.7147	0.7210	0.7155
	2	0.7249	0.7319	0.7253	0.7243
	3	0.8923	0.8905	0.8931	0.8912
	4	0.8645	0.8652	0.8649	0.8627
	5	0.8775	0.8811	0.8781	0.8780
	6	0.8486	0.8468	0.8494	0.8475
LSTM	1	0.8152	0.8152	0.8195	0.8125
	2	0.8219	0.8219	0.8375	0.8161
	3	0.9384	0.9384	0.9385	0.9380
	4	0.9346	0.9346	0.9349	0.9345
	5	0.9362	0.9362	0.9375	0.9356
	6	0.8962	0.8962	0.8963	0.8958
GRU	1	0.8130	0.8130	0.8415	0.8080
	2	0.8519	0.8518	0.8528	0.8504
	3	0.9425	0.9420	0.9427	0.9420
	4	0.9392	0.9392	0.9397	0.9385
	5	0.9398	0.9398	0.9413	0.9395
	6	0.9035	0.9030	0.9037	0.9030

The confusion matrix in Fig. 8 (b) indicates high accuracy for nine compound sitting actions across all algorithms. LSTM and GRU stand out, achieving above 95% accuracy for most actions, except MR. Conversely, SVM, while effective for certain actions, exhibits limited accuracy in swing operations, MR, and RL Boom. This limitation stems from the extended duration of most sitting actions, involving overlapping static postures. Traditional machine learning with fixed sliding windows excels in consistent activity recognition but struggles with compound action transitions. Deep learning algorithms like LSTM and GRU, are useful for capturing long-term time series dependencies and significantly enhance compound sitting actions classification.

Subsequent analysis highlights lower prediction accuracies for swing operations (accuracy: SVM: 87%, LSTM: 82%, GRU: 83%) across all algorithms. This is likely due to the excavator's significant movement range during these operations, causing marked fluctuations in pressure sensors and IMUs signals, which complicates classification. The results also found that the predictive accuracy of LSTM and GRU for MR is limited, with some MRs being incorrectly classified as swing operations. This may be attributed to the fact that, during the execution of MR, there is a prolonged period where the motion resembles that of a swing operation, characterized by a tendency to rotate the fuselage to the right. Consequently, the operator's actions in both scenarios exhibit certain similarities.

As illustrated in Fig. 8 (b), based on the ROC curves of the three algorithms for various classifications, the majority of AUC values exceeded 0.95, indicating the effectiveness of the classifiers. For swing operations, MR, RL Boom, SVM classifier achieved the smallest AUC value of 0.97, suggesting slightly lower prediction accuracy for these three categories. This observation aligns with the analysis conducted on the confusion matrix.

Fig. 9 (b) displays the performance of the GRU under scheme #3 in terms of accuracy and loss curves. Similar to the performance of the model in a static sitting posture, the GRU achieves convergence in both accuracy and loss. This indicates that the GRU model has undergone effective training and has successfully avoided overfitting.

In this paper, a balanced dataset was used to accurately capture the characteristics of excavator operators' sitting activities. However, to further demonstrate the reliability and generalization of the developed models in recognizing sitting activities, imbalanced datasets that are closer to real excavator operations than controlled field experimental datasets are required. To this end, an imbalance processing was introduced to the original test set. The previously trained model was tested using these imbalanced data and compared with the recognition performance on the original test set. This model evaluation approach has been widely used in the construction industry [118]. To align the activity duration and sequence more closely with real excavation scenarios, insights from earthwork field surveys were combined with relevant existing studies [119-121]. An imbalanced dataset was constructed through data augmentation, with the following activity sequence: MF (30s), ML (10s), Climbing (10s), RL Boom (6.25s), RL Arm (6.25s), Excavation (30s), Swing (3s), Dumping (5s), MR (10s). The original dataset was cropped to extract the time series of each activity based on the predefined duration. Linear interpolation was applied between continuous compound sitting actions to ensure a smoother dataset, followed by downsampling to maintain a consistent sampling frequency in the generated imbalanced dataset. Techniques of jittering and rotation were adopted to emulate the random noise generated during excavator operation and the potential orientation shifts in IMUs caused by vibrations and movements. The jittering was applied to the pressure sensors dataset, while both jittering and rotation were implemented on the IMUs dataset. The noise was modeled using common Gaussian white noise, and the rotation angle was set at 5 degrees [122]. Based on the preceding results, the SVM, LSTM, and GRU algorithms demonstrated relatively optimal accuracy in recognizing compound sitting actions. Consequently, the activity recognition performance evaluation of these three algorithms was further conducted. Specific performance metrics are shown in

Fig. 10.

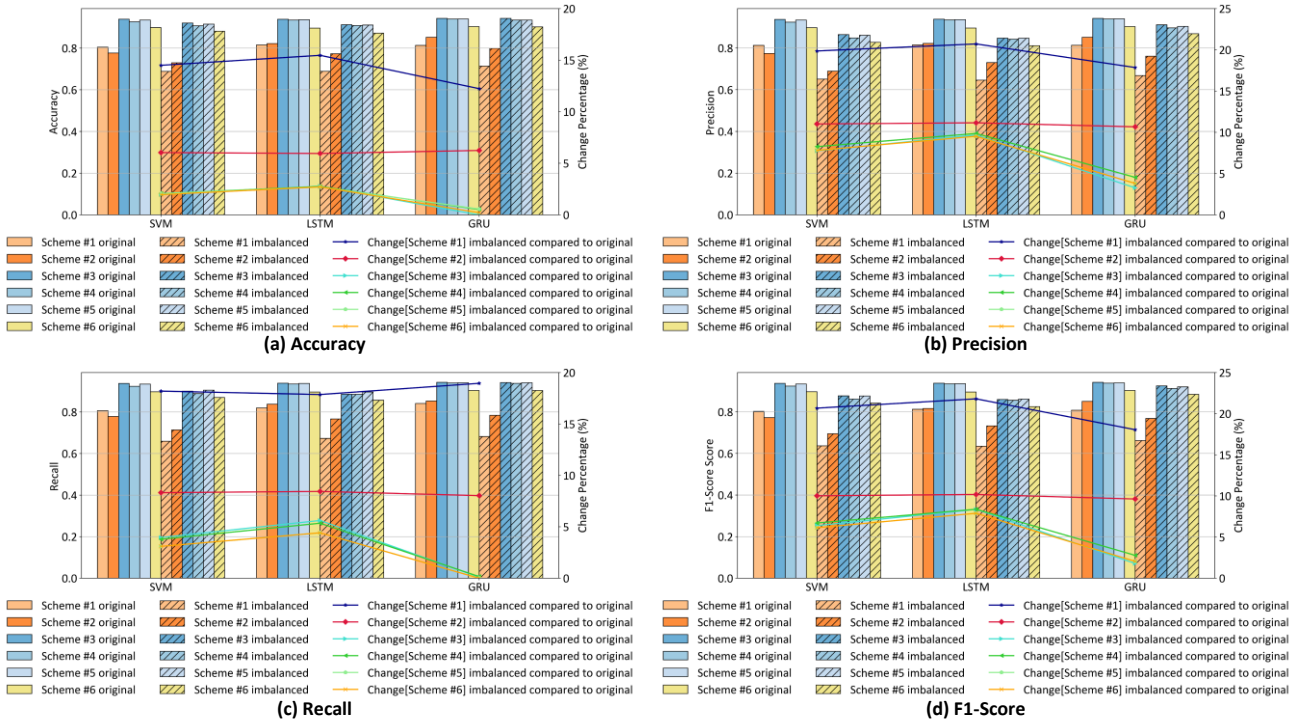

Fig. 10. Comparison of model performance metrics under original and imbalanced dataset.

The performance metrics presented in Fig. 10 reveal variations across different models when applied to the imbalanced dataset. Particularly, relying solely on pressure sensors resulted in a decline in performance, ranging from 12.23% to 21.80% compared to the original dataset. This outcome underscores the limitations of activity recognition reliant on a single type of sensor, especially when processing imbalanced datasets that resemble real-world constructions. As such, pressure sensors are more susceptible to interference from noise and other factors. However, when employing a multi-sensor combination strategy, the decline in performance metrics is significantly mitigated (ranging from 0.03% to 9.68%). Notably, scheme #6 demonstrates equally superior efficacy in managing imbalanced datasets (ranging from 0.02% to 9.53%). These findings substantiate the advantage of the multi-sensor combination approach for operators' sitting activity recognition, demonstrating its robust adaptability in the complex operational environments of construction sites. Regarding individual algorithms, GRU consistently outperforms others in both datasets, further confirming the superior generalization performance of deep learning algorithms.

4.2. Comparison of multi-sensor combination schemes

In real construction sites, the complex operating environments and application requirements for sensors (e.g., cost,

invasiveness) may necessitate different configurations of multi-sensor setups. Thus, this paper conducts a detailed comparison of recognition performance using the multi-sensor combination scheme proposed earlier. Table 6 presents the performance metrics for the recognition of excavator operator's sitting postures under various multi-sensor combinations. These metrics represent the average values of all algorithm performance indicators for each combination scheme.

Table 6 Average recognition performance for static sitting postures across each multi-sensor combination scheme.

#	Combination schemes	Performance metrics			
		Accuracy	**Precision**	**Recall**	**F1-Score**
1	Only use pressure sensors	0.8584	0.8611	0.8581	0.8579
2	Only use IMUs	0.9283	0.9286	0.9284	0.9282
3	Fusion of pressure sensors and all IMUs	0.9625	0.9645	0.9625	0.9623
4	Fusion of pressure sensors and the IMU at the torso	0.9533	0.9532	0.9531	0.9529
5	Fusion of pressure sensors and the IMUs at the arms	0.9548	0.9566	0.9547	0.9564

As depicted in Table 6, higher recognition performance for static sitting postures can be achieved with fewer sensor combinations, such as "only using pressure sensors" or "only using IMUs." The accuracy improves to some extent by fusing pressure sensors and IMUs. Interestingly, the placement of IMUs (e.g., at the torso or arms) seems to have an impact on recognition performance. This outcome can be attributed to the noticeable changes in the body torso during different static sitting postures and the significant differences in data between IMUs placed at the torso and the arms. SVM and GRU algorithms demonstrate strong performance in the classification of static sitting postures. Therefore, the subsequent analysis will utilize SVM and GRU algorithms to further examine the confusion matrix under different multi-sensor combination schemes.

Fig. 11 (a) shows SVM's recognition accuracy for LR is only 54% when relying solely on pressure sensors. This is attributed to the similar pressure distribution in LR and CLL postures and potential data quality reduction due to the operator's movement during LR data gathering. Conversely, IMUs do not encounter this issue, as they distinctly capture the varying torso orientations of LR and CLL. Moreover, Fig. 11 (a) and (b) indicate poor classification accuracy for LB by both algorithms. This discrepancy arises due to the confined space in the operation room, resulting in minimal forward or backward leaning amplitudes of the operator's torso. Further examination of Fig. 11 (c) and (d) shows clear misclassifications of SU and CLL by both algorithms when solely utilizing IMUs. These errors likely arise from the postures' relatively vertical torso and minimal movement amplitudes, complicating accurate differentiation.

As depicted in Fig. 11 (e) and (f), when fusing all IMUs and pressure sensors, both algorithms demonstrate excellent accuracy for various static sitting postures, with SVM achieving 95.69% and GRU achieving 98.50%. Notably, when fusing pressure sensors with the IMU at the torso, SVM exhibits exceptional differentiation for static sitting postures. However, the distinction for LR is relatively lower (88% accuracy), possibly due to the limited space in the operational area, which constrains the extent of the operator's overall leaning movements, leading to reduced sensitivity in the torso's IMU data, consequently making it challenging to distinguish from other static sitting postures. Furthermore, fusing pressure sensors with arm IMUs led to SVM and GRU algorithms nearly replicating the performance levels attained with full IMU utilization.

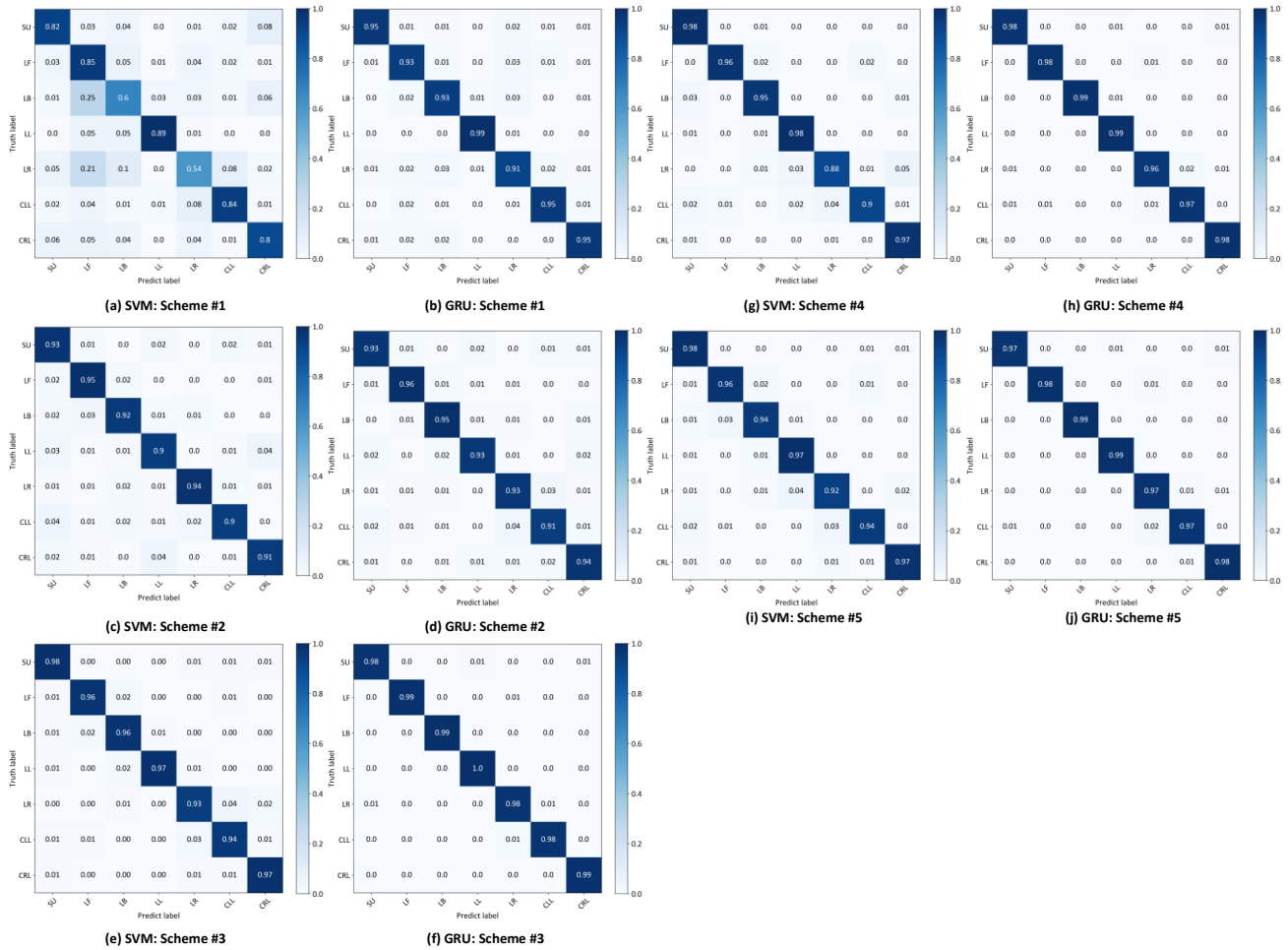

Fig. 11. Confusion matrix of static sitting posture under SVM and GRU.

Table 7 presents the average performance metrics for the recognition of compound sitting actions under different sensor combination schemes. It is evident that both the "only use pressure sensors" and "only use IMUs" schemes achieve a certain level of accuracy in classifying compound sitting actions, while the fusion of multiple sensors significantly enhances recognition performance. The accuracy of fusing pressure sensors with IMUs at the arms was

slightly higher compared to fusing pressure sensors with IMUs at the torso. This finding can be attributed to the distinct range of changes in the IMUs at the arms and the accurate classification of various compound sitting actions. Furthermore, the fusion of pressure sensors with IMUs on the excavator seat side wall also demonstrates significantly improved classification accuracy compared to using a single sensor, although its accuracy remains lower than that of the fusion of all sensors.

Table 7 Average recognition performance for compound sitting actions across each multi-sensor combination scheme.

#	Combination schemes	Performance metrics			
		Accuracy	**Precision**	**Recall**	**F1-Score**
1	Only use pressure sensors	0.7866	0.7890	0.7903	0.7842
2	Only use IMUs	0.7884	0.7901	0.7972	0.7868
3	Fusion of pressure sensors and all IMUs	0.9229	0.9221	0.9228	0.9220
4	Fusion of pressure sensors and the IMU at the torso	0.9096	0.9095	0.9096	0.9086
5	Fusion of pressure sensors and the IMUs at the arms	0.9150	0.9157	0.9157	0.9148
6	Fusion of pressure sensors and the IMU at excavator seat side wall	0.8816	0.8808	0.8815	0.8807

Analysis of Fig. 12 (a) and (b) reveals that when only pressure sensors are used, GRU (71% accuracy) exhibits the lowest accuracy in recognizing excavation operations. This misclassification can be attributed to the operator's limited movement of the upper and lower arms during excavation operations, resulting in minimal changes in both the excavator and human torso. Consequently, the pressure sensor data does not exhibit significant variations. Moreover, the subtle changes in pressure data during complex compound sitting actions like excavation, dumping, and climbing lead to generally low classification accuracies across algorithms. Particularly, SVM's performance in classifying ML, MR, and swing operation is diminished, attributed to its reduced efficacy in transitional data recognition. The fuselage's left-right oscillation during swing operations also mimics the pressure patterns of ML and MR, complicating accurate identification.

However, as depicted in Fig. 12 (c) and (d), when only IMUs were used, the previously low classification accuracy, primarily caused by the complexity and specificity of arm movements, significantly improved. Nevertheless, the SVM algorithm demonstrates the lowest accuracy (74% accuracy) for the climbing operation, with 24% of the data being incorrectly classified as RL Boom. This misclassification arises due to the operator's reliance on using the Boom to stabilize the fuselage for uphill tasks during climbing operations. Consequently, both of these compound sitting actions involve extensive use of the Boom control lever.

Fig. 12 (e) and (f) illustrate that the fusion of pressure sensors and IMUs significantly improves the algorithm's

performance in recognizing compound sitting actions. By comparing Fig. 12 (g-j), no significant difference in recognition accuracy was observed between fusing pressure sensors with IMUs at the arms and using all IMUs. However, the recognition accuracy of fusing pressure sensors with IMUs at the torso slightly decreases. This decline can be attributed to the IMU at the torso being adhered to the operator's body, resulting in less overall movement compared to the arms.

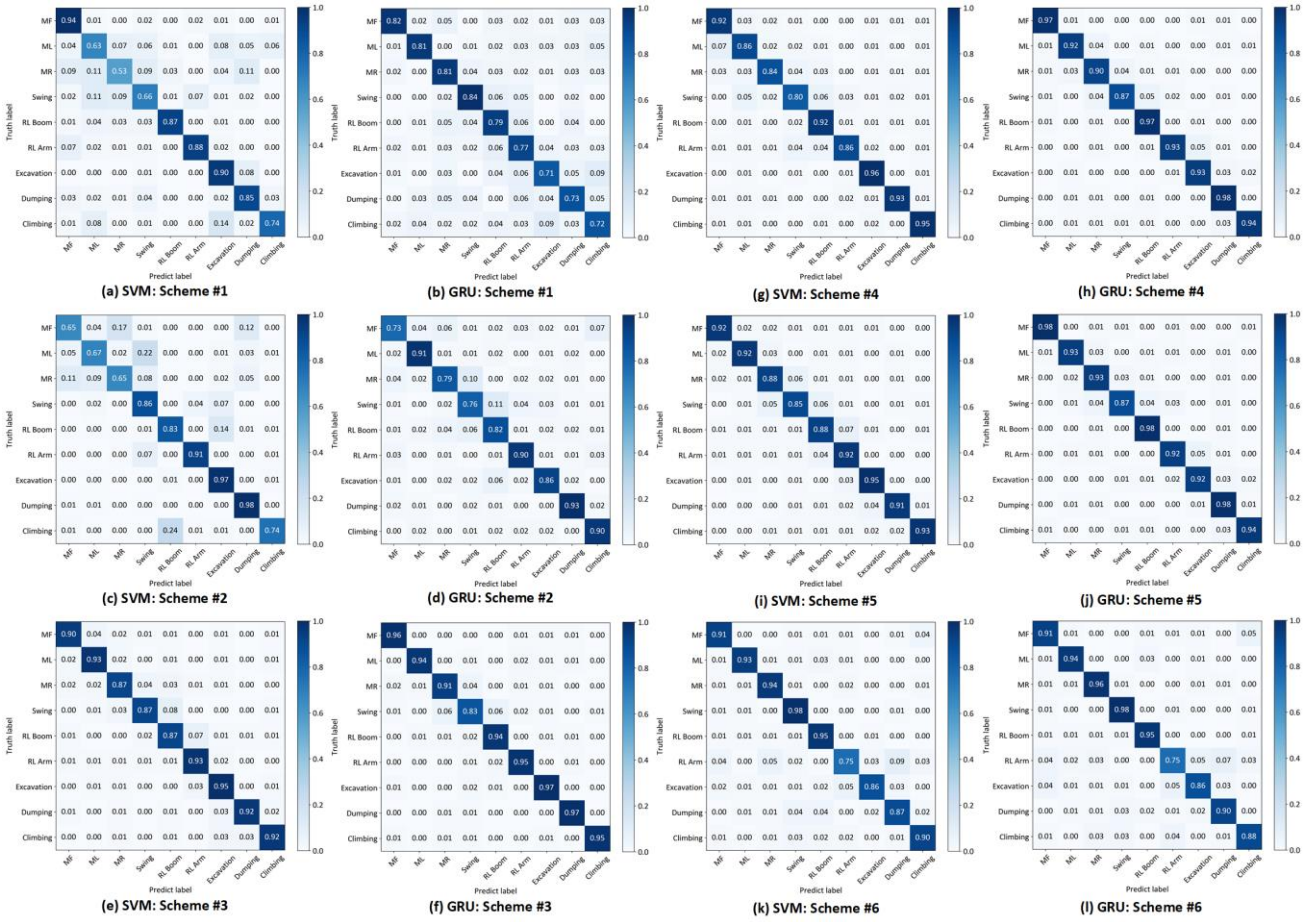

Fig. 12. Confusion matrix of compound sitting actions under SVM and GRU.

5. Discussion

5.1. Feasibility of the proposed methods

The proposed method was applied in excavator operation scenarios, demonstrating its feasibility for recognizing operators' sitting activities. The results indicated that the selected algorithms achieved satisfactory performance in recognizing sitting activities across various multi-sensor combinations. For static sitting postures, excellent performance was observed across different algorithms, with all performance evaluation indicators exceeding 90%

when using the complete multi-sensor combination. Among these, the machine learning algorithms demonstrated similar performance, while the two deep learning algorithms showed only marginal improvements compared to the machine learning algorithms. Overall, the distinction in recognition performance between the two types of algorithms was not substantial. For compound sitting actions, the performance indicators of LSTM and GRU surpassed 80% for various sitting actions under different multi-sensor combinations. Notably, GRU consistently exhibited outstanding recognition performance, indicating its high potential for detecting sitting activities of excavator operators. Additionally, when using a single sensor, the performance of the three machine learning algorithms was comparable. With the combination of multiple sensors, the performance indicators of SVM significantly outperformed the other two algorithms. Overall, the performance of machine learning algorithms in compound sitting actions recognition was notably lower than that of the two deep learning algorithms. Moreover, through model testing and evaluation on the imbalanced dataset that closely resembles actual excavation operations, this paper demonstrates the acceptable reliability and generalization of the proposed method to a certain extent. Among these, GRU demonstrated the best performance in terms of training time and overall recognition accuracy. These findings highlight the applicability and feasibility of the selected RNN-based algorithms for processing time series data of excavator operators' sitting activities.

The proposed method demonstrated distinct differences in recognizing static sitting postures and compound sitting actions. In the recognition of static sitting postures, all different sensor combination approaches exhibit acceptable classification accuracy. This finding can be attributed to the significant changes in the operator's center of gravity across different static sitting postures, which can be precisely captured. The position of the torso and the corresponding interface pressure distribution vary noticeably among different sitting postures, enabling the identification of static sitting postures using only a single sensor. However, in the recognition of compound sitting actions, the performance of a single interface pressure sensor array is inferior to that of the multi-sensor combination approach. When only employing IMUs, the algorithm's performance shows a slight improvement compared to using only the interface pressure sensor. Nevertheless, the overall recognition performance remains relatively low and can potentially disrupt the operation process due to its invasive nature. The sitting actions of excavator operators involve a multitude of compound body movements, but operators typically maintain a relatively upright sitting posture during

operation. As a result, the pressure distribution does not exhibit significant changes between different sitting actions, thereby resulting in poor recognition performance. These challenges emphasize the complexity and dynamics associated with the operators sitting activities.

The utilization of the multi-sensor combination schemes has significantly enhanced the practicability and recognition performance of the method. Notably, the highest recognition performance was achieved when all sensors were used. When fusing the interface pressure sensor data with arm-mounted IMU data, the recognition accuracy slightly surpassed that of the approach combining the pressure sensor with the torso-mounted IMU. This observation may be attributed to the pronounced overall range of arm movements across various sitting activities, with the arm-mounted IMUs providing more precise data on the operator's arm movements. However, this solution may introduce invasive effects and inconveniences associated with wearing arm-mounted sensors. It is worth mentioning that the combination of the pressure sensor array and the IMU installed on the seat exhibited considerable recognition performance. Since the IMU is integrated into the excavator's structure, it does not interfere with the operator's regular work while capturing equipment movement. Consequently, it represents a compromise approach that balances recognition performance with practical considerations such as cost and intrusiveness. Overall, the results demonstrated that relying solely on the pressure sensor array yields significantly lower recognition performance compared to multi-sensor fusion. In particular, when the IMU is positioned on the excavator structure, this scheme exhibits considerable applicability to other construction equipment operation scenarios. This finding further indicates that when the operator's sitting activities are influenced by equipment movement, the employed sensors may receive corresponding noise signals, thereby compromising the data quality. The proposed method could simultaneously capture both irregular equipment movements and corresponding operators' sitting activity information through multi-sensor fusion. Compared with using operator sitting activity-related data alone, this multi-sensor data fusion approach demonstrates superior sitting activity recognition performance.

5.2. Contributions and implications to theory and construction practice

This paper develops theoretical methods and technical solutions for excavator operator activity recognition. The collection of kinematics-based data in real construction task scenarios presents significant challenges due to the

construction site's complex, dynamic, and harsh environmental factors. Moreover, previous studies primarily relied on data collected from laboratory experiments, which limits the evaluation of the usability and reliability of sensing technology and data processing methods in practical settings. To overcome these limitations, this paper conducts experiments and collects data in a real construction site environment. By integrating interface pressure sensing technology and IMU sensors, simultaneous real-time collection of excavator operators' sitting activities and corresponding equipment movement data becomes possible. Consequently, the complex dynamics of operator activities, influenced by the irregular movements of construction equipment, can be comprehensively recorded and effectively reflected in the generated features. This supports the selected algorithms in achieving acceptable recognition performance. The proposed approach exhibits the potential for extension to a broader range of heavy machinery operating scenarios in challenging and dynamic task environments. Specifically, the proposed method offers the following advantages:

(1) Multiple sensors were employed to enable the simultaneous collection of target signals and noise signals from both the equipment and operators, facilitating the comprehensive recording of the entire construction equipment operating scenario. The findings demonstrate that satisfactory recognition outcomes can be attained by combining the interface pressure sensor array with a reduced number of IMUs. This presents a fundamental hardware technical solution for addressing activity recognition challenges in dynamic construction equipment operation scenarios.

(2) This paper compared various machine learning and deep learning algorithms for the recognition of excavator operator activities. The results unequivocally indicated that RNN-based algorithms are highly effective in capturing the dynamic characteristics of time series data, exhibiting greater suitability for addressing the research problem. Notably, GRU consistently exhibited superior recognition performance in certain cases, even when utilizing a reduced number of sensors.

(3) Operators' sitting activity recognition methods with high adaptability can be developed by employing flexible combinations of multiple sensors. Considering practical requirements such as cost-effectiveness and non-intrusiveness, distinct schemes for multi-sensor combinations are proposed, and their feasibility is validated. This allows for the customization of multi-sensor combinations to suit diverse project requirements and construction site conditions. In real-world applications, suitable approaches can be selected by carefully considering the trade-off

between application practicability and efficiency.

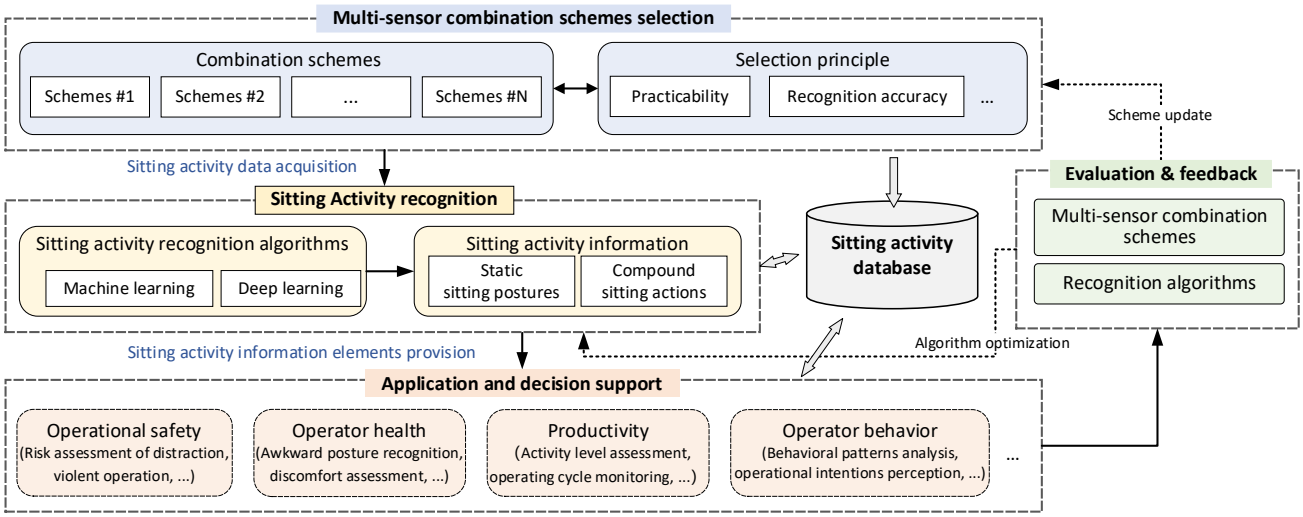

Fig. 13. Practical use of the research.

Furthermore, the proposed method holds potential as a real-time sitting activities recognition tool for managing the performance of construction equipment operators. To facilitate practical implementation, an executable application framework was developed, as illustrated in Fig. 13. First, an appropriate multi-sensor combination scheme should be selected, considering a trade-off between practicability and recognition performance. This selection process should account for specific application scenario characteristics, activity recognition objectives, project cost control, and other relevant factors. The collected data incorporates several interpretable interface pressure metrics, which provide quantitative information on sitting activities. The feedback outcomes can facilitate various aspects of on-site management, thereby offering significant implications for operator management practices. The information generated can be utilized for proactive safety risk analysis, health risk assessment, predictive productivity evaluation, and integration into data-driven methodologies for operators' behavior perception and operational situation awareness. For example, the developed method can serve as a technical foundation for measuring and evaluating operators' physical discomfort and muscle fatigue levels during prolonged sitting situations, elucidating changes in sitting posture through pressure distribution and related inertial indicators. Additionally, the evaluation of the recognition results can inform improvements in the sensor combination scheme and the recognition algorithm. While the specific application of this framework extends beyond the scope of this paper, its potential benefits are worth exploring in future research and implementation endeavors.

5.3. Limitations and future research directions

In construction project practice, the configuration of multiple sensors necessitates a trade-off between method efficiency and practicability costs. In this paper, a 15×17 pressure sensor array was utilized, which is a redundant sensor arrangement scheme. The purpose was to fully explore the feasibility of interface pressure sensing technology. Consequently, some parts of the pressure sensor units in the sensor array did not encounter the participant's body in most cases. From the perspective of pressure sensor unit distributions, the pressure features captured by multiple sensor units in a ROI may be effectively represented by a particular sensor unit within that region. This observation presents a potential basis for optimizing the layout of the pressure sensor array. Future research should focus on developing rational sensor layout optimization methods while achieving acceptable sitting activity recognition performance across a broader range of construction equipment operation scenarios, including its accuracy, generalization, and other relevant factors. Furthermore, regarding multi-sensor fusion methods, this paper falls under the category of feature-level fusion method [32]. To enhance the practicability of the multi-sensor systems in diverse operational tasks, it is crucial to gather more training data in a real construction environment and explore various data fusion methods regarding their feasibility, adaptability, and recognition performance. Finally, it is important to acknowledge that this paper employed a partially controlled field experimental setup, although ensuring a balanced dataset and experimental safety, may not fully capture the complexities of real-world construction scenarios. Hence, the practicability of the proposed method is still subject to certain limitations. To address this, future research efforts should verify the reliability of the proposed method under completely uncontrolled conditions, which may necessitate the development of efficient signal processing techniques and robust classification algorithms.

6. Conclusions

This paper collected and recognized excavator operators' sitting activities in construction equipment operating environments. The outcomes could provide essential insights for managing health and safety risks and improving production efficiency on construction sites. To this end, a field experiment was conducted on a real-world construction site to collect multi-sensor data on static sitting postures and compound sitting actions in real excavator operating scenarios. A multi-sensor system, consisting of two pressure sensor arrays and four IMUs sensors, was

759 developed to comprehensively capture the dynamics of the excavator operator's sitting posture. To systematically
760 describe the characteristics of the interface pressure during operating activities, several typical metrics were generated,
761 and corresponding features were extracted. The results demonstrated that several machine learning and deep learning
762 algorithms, including SVM and GRU, achieved superior recognition performance. Specifically, the accuracy of
763 recognizing compound sitting actions ranges from 77.66% to 93.46% across multi-sensor combinations using SVM,
764 and from 81.30% to 94.25% using GRU. This paper also explored the recognition performance across different sensor
765 combinations, highlighting the feasibility and adaptability of various algorithms and sensor combinations in diverse
766 scenarios.

767 This paper contributes to both theory and practice in the following ways: (1) The interface pressure sensing
768 technique and effective pressure indicators related to the excavator operator's sitting activity are proposed, and its
769 feasibility is demonstrated. (2) Through multi-sensor data fusion, the construction equipment movements and the
770 complex dynamics of excavator operators' sitting activities affected by irregular equipment movements can be
771 synchronously captured. This mitigates the adverse effects of equipment vibration and movement on operators' sitting
772 activity recognition performance, making the proposed method suitable for construction operation contexts. (3)
773 Comparative analysis of field experimental results identified suitable activity recognition methods that could
774 recognize excavator operators' static sitting postures and compound sitting actions. (4) The performance of sitting
775 activity recognition under various sensor combinations was compared, and optimized sensor arrangement schemes
776 adaptable to various on-site construction operation scenarios were preliminarily discussed. Moreover, it was revealed
777 that for more general problems of activity detection and recognition in complex construction equipment operation
778 scenarios, a multi-sensor fusion-based approach could be a promising technical solution. Future research should focus
779 on optimizing multi-sensor arrangements and investigating the feasibility and practicability of the proposed methods
780 across various real construction equipment operation scenarios.

781 ## Acknowledgments

782 This work was partially supported by the National Natural Science Foundation of China (No. 72201254), the
783 Project funded by China Postdoctoral Science Foundation (No. 2021M692990), the General Research Fund (GRF)

Grant (No. 15201621, 15210923), and the Shenzhen Fundamental Research Program (Grant No. SGDX20201103095203031). Finally, we would like to express our sincere gratitude to the reviewers for their valuable comments and suggestions on the improvement of the research quality.

References

[1] X. Shen, I. Awolusi, E. Marks, Construction equipment operator physiological data assessment and tracking, Practice Periodical on Structural Design and Construction. 22 (4) (2017), pp. 04017006, https://doi.org/10.1061/(asce)sc.1943-5576.0000329.

[2] V.H.P. Vitharana, T. Chinda, Development of a lower back pain prevention index for heavy equipment operators in the construction industry: system dynamics modelling, International Journal of Construction Management. (2019), pp. 1-17, https://doi.org/10.1080/15623599.2019.1579969.

[3] N.K. Kittusamy, B. Buchholz, Whole-body vibration and postural stress among operators of construction equipment: a literature review, Jounal of Safety Research. 35 (3) (2004), pp. 255-261, https://doi.org/10.1016/j.jsr.2004.03.014.

[4] M.P. Smets, T.R. Eger, S.G. Grenier, Whole-body vibration experienced by haulage truck operators in surface mining operations: a comparison of various analysis methods utilized in the prediction of health risks, Applied Ergonomics. 41 (6) (2010), pp. 763-770, https://doi.org/10.1016/j.apergo.2010.01.002.

[5] T. Waters, A. Genaidy, H. Barriera Viruet, M. Makola, The impact of operating heavy equipment vehicles on lower back disorders, Ergonomics. 51 (5) (2008), pp. 602-636, https://doi.org/10.1080/00140130701779197.

[6] J. Li, H. Li, H. Wang, W. Umer, H. Fu, X. Xing, Evaluating the impact of mental fatigue on construction equipment operators' ability to detect hazards using wearable eye-tracking technology, Automation in Construction. 105 (2019), pp. 102835, https://doi.org/10.1016/j.autcon.2019.102835.

[7] I. Mehmood, H. Li, Y. Qarout, W. Umer, S. Anwer, H. Wu, M. Hussain, M. Fordjour Antwi-Afari, Deep learning-based construction equipment operators' mental fatigue classification using wearable EEG sensor data, Advanced Engineering Informatics. 56 (2023), pp. 101978, https://doi.org/10.1016/j.aei.2023.101978.

[8] S.K.K. Jeripotula, A. Mangalpady, G.R.R. Mandela, Assessment of exposure to whole-body vibration of dozer operators based on postural variability, Mining Metallurgy & Exploration. 37 (2) (2020), pp. 813-820, https://doi.org/10.1007/s42461-020-00175-z.

[9] K. Ramar, L.A. Kumaraswamidhas, Excavator driver seat occupational comfort assessment with lumbar support cushion, Journal of Vibration and Control. 28 (23-24) (2021), pp. 3510-3523, https://doi.org/10.1177/10775463211035891.

[10] J.S. Lee, Y. Ham, H. Park, J. Kim, Challenges, tasks, and opportunities in teleoperation of excavator toward human-in-the-loop construction automation, Automation in Construction. 135 (2022), pp. 104119, https://doi.org/10.1016/j.autcon.2021.104119.

[11] A.S. Rao, M. Radanovic, Y. Liu, S. Hu, Y. Fang, K. Khoshelham, M. Palaniswami, T. Ngo, Real-time monitoring of construction sites: Sensors, methods, and applications, Automation in Construction. 136 (2022), pp. 104099, https://doi.org/10.1016/j.autcon.2021.104099.

[12] P.B. Rodrigues, R. Singh, M. Oytun, P. Adami, P.J. Woods, B. Becerik-Gerber, L. Soibelman, Y. Copur-Gencturk, G.M. Lucas, A multidimensional taxonomy for human-robot interaction in construction, Automation in Construction. 150 (2023), pp. 104845, https://doi.org/10.1016/j.autcon.2023.104845.

[13] B. Sherafat, C.R. Ahn, R. Akhavian, A.H. Behzadan, M. Golparvar-Fard, H. Kim, Y.-C. Lee, A. Rashidi, E.R. Azar, Automated methods for activity recognition of construction workers and equipment: State-of-the-art review, Journal of Construction Engineering and Management. 146 (6) (2020), pp. 03120002, https://doi.org/10.1061/(asce)co.1943-

7862.0001843.
[14] Y. Yu, W. Umer, X. Yang, M.F. Antwi-Afari, Posture-related data collection methods for construction workers: A review, Automation in Construction. 124 (2021), pp. 103538, https://doi.org/10.1016/j.autcon.2020.103538.
[15] T. Cheng, J. Teizer, G.C. Migliaccio, U.C. Gatti, Automated task-level activity analysis through fusion of real time location sensors and worker's thoracic posture data, Automation in Construction. 29 (2013), pp. 24-39, https://doi.org/10.1016/j.autcon.2012.08.003.
[16] L. Minh Dang, K. Min, H. Wang, M. Jalil Piran, C. Hee Lee, H. Moon, Sensor-based and vision-based human activity recognition: A comprehensive survey, Pattern Recognition. 108 (2020), pp. 107561, https://doi.org/10.1016/j.patcog.2020.107561.
[17] C.R. Ahn, S. Lee, C. Sun, H. Jebelli, K. Yang, B. Choi, Wearable sensing technology applications in construction safety and health, Journal of Construction Engineering and Management. 145 (11) (2019), pp. 03119007, https://doi.org/10.1061/(asce)co.1943-7862.0001708.
[18] J.C.T. Mallare, D.F.G. Pineda, G.M. Trinidad, R.D. Serafica, J.B.K. Villanueva, A.R. Dela Cruz, R.R.P. Vicerra, K.K.D. Serrano, E.A. Roxas, Sitting posture assessment using computer vision, 2017 IEEE 9th International Conference on Humanoid, Nanotechnology, Information Technology, Communication and Control, Environment and Management (HNICEM), Manila, Philippines, 2017, pp. 1-5, https://doi.org/10.1109/HNICEM.2017.8269473.
[19] G. Liang, J. Cao, X. Liu, Smart cushion: A practical system for fine-grained sitting posture recognition, 2017 IEEE International Conference on Pervasive Computing and Communications Workshops, Kona, HI, USA, 2017, pp. 419-424, https://doi.org/10.1109/PERCOMW.2017.7917599.
[20] A. Arrogi, A. Bogaerts, J. Seghers, K. Devloo, V. Vanden Abeele, L. Geurts, J. Wauters, F. Boen, Evaluation of stAPP: a smartphone-based intervention to reduce prolonged sitting among Belgian adults, Health promotion international. 34 (1) (2019), pp. 16-27, https://doi.org/10.1093/heapro/dax046.
[21] C.-C. Wu, C.-C. Chiu, C.-Y. Yeh, Development of wearable posture monitoring system for dynamic assessment of sitting posture, Physical and Engineering Sciences in Medicine. 43 (1) (2019), pp. 187-203, https://doi.org/10.1007/s13246-019-00836-4.
[22] M. Stinson, R. Ferguson, A. Porter-Armstrong, Exploring repositioning movements in sitting with ‘at risk’ groups using accelerometry and interface pressure mapping technologies, Journal of Tissue Viability. 27 (1) (2018), pp. 10-15, https://doi.org/10.1016/j.jtv.2017.11.001.
[23] N. Akkarakittichoke, P. Janwantanakul, Seat pressure distribution characteristics during 1 hour sitting in office workers with and without chronic low back pain, Safety and Health at Work. 8 (2) (2017), pp. 212-219, https://doi.org/10.1016/j.shaw.2016.10.005.
[24] R. Zemp, M. Fliesser, P.M. Wippert, W.R. Taylor, S. Lorenzetti, Occupational sitting behaviour and its relationship with back pain - A pilot study, Applied Ergonomics. 56 (2016), pp. 84-91, https://doi.org/10.1016/j.apergo.2016.03.007.
[25] W. Kim, B. Jin, S. Choo, C.S. Nam, M.H. Yun, Designing of smart chair for monitoring of sitting posture using convolutional neural networks, Data Technologies and Applications. 53 (2) (2019), pp. 142-155, https://doi.org/10.1108/dta-03-2018-0021.
[26] W. Li, S. Yu, H. Yang, H. Pei, C. Zhao, Effects of long-duration sitting with limited space on discomfort, body flexibility, and surface pressure, International Journal of Industrial Ergonomics. 58 (2017), pp. 12-24, https://doi.org/10.1016/j.ergon.2017.01.002.
[27] C. Ma, W. Li, R. Gravina, G. Fortino, Posture detection based on smart cushion for wheelchair users, Sensors. 17 (4) (2017), https://doi.org/10.3390/s17040719.
[28] G. Kyung, M.A. Nussbaum, Driver sitting comfort and discomfort (part II): Relationships with and prediction from interface pressure, International Journal of Industrial Ergonomics. 38 (5-6) (2008), pp. 526-538, https://doi.org/10.1016/j.ergon.2007.08.011.

[29] J.M. Porter, D.E. Gyi, H.A. Tait, Interface pressure data and the prediction of driver discomfort in road trials, Applied Ergonomics. 34 (3) (2003), pp. 207-214, https://doi.org/10.1016/s0003-6870(03)00009-7.
[30] J. Cheng, M. Sundholm, B. Zhou, M. Hirsch, P. Lukowicz, Smart-surface: Large scale textile pressure sensors arrays for activity recognition, Pervasive and Mobile Computing. 30 (2016), pp. 97-112, https://doi.org/10.1016/j.pmcj.2016.01.007.
[31] H.F. Nweke, Y.W. Teh, G. Mujtaba, M.A. Al-garadi, Data fusion and multiple classifier systems for human activity detection and health monitoring: Review and open research directions, Information Fusion. 46 (2019), pp. 147-170, https://doi.org/10.1016/j.inffus.2018.06.002.
[32] S. Qiu, H. Zhao, N. Jiang, Z. Wang, L. Liu, Y. An, H. Zhao, X. Miao, R. Liu, G. Fortino, Multi-sensor information fusion based on machine learning for real applications in human activity recognition: State-of-the-art and research challenges, Information Fusion. 80 (2022), pp. 241-265, https://doi.org/10.1016/j.inffus.2021.11.006.
[33] R. Gravina, P. Alinia, H. Ghasemzadeh, G. Fortino, Multi-sensor fusion in body sensor networks: State-of-the-art and research challenges, Information Fusion. 35 (2017), pp. 68-80, https://doi.org/10.1016/j.inffus.2016.09.005.
[34] S. Miao, L. Chen, R. Hu, Y. Luo, Towards a dynamic inter-sensor correlations learning framework for multi-sensor-based wearable human activity recognition, Proceedings of the ACM on Interactive, Mobile, Wearable and Ubiquitous Technologies. 6 (3) (2022), pp. 1-25, https://doi.org/10.1145/3550331.
[35] Y. Zhou, Z. Yang, X. Zhang, Y. Wang, A hybrid attention-based deep neural network for simultaneous multi-sensor pruning and human activity recognition, IEEE Internet of Things Journal. 9 (24) (2022), pp. 25363-25372, https://doi.org/10.1109/jiot.2022.3196170.
[36] J. Cao, W. Li, C. Ma, Z. Tao, Optimizing multi-sensor deployment via ensemble pruning for wearable activity recognition, Information Fusion. 41 (2018), pp. 68-79, https://doi.org/10.1016/j.inffus.2017.08.002.
[37] Y. Zeng, C. Wang, C.-C. Chen, W.-P. Xiong, Z. Liu, Y.-C. Huang, C. Shen, Smart device monitoring system based on multi-type inertial sensor machine learning, Sensors and Materials. 33 (2) (2021), pp. 693-714, https://doi.org/10.18494/sam.2021.3037.
[38] M.F. Antwi-Afari, H. Li, J.K.-W. Wong, O.T. Oladinrin, J.X. Ge, J. Seo, A.Y.L. Wong, Sensing and warning-based technology applications to improve occupational health and safety in the construction industry, Engineering, Construction and Architectural Management. 26 (8) (2019), pp. 1534-1552, https://doi.org/10.1108/ecam-05-2018-0188.
[39] C. Craye, A. Rashwan, M.S. Kamel, F. Karray, A multi-modal driver fatigue and distraction assessment system, International Journal of Intelligent Transportation Systems Research. 14 (3) (2015), pp. 173-194, https://doi.org/10.1007/s13177-015-0112-9.
[40] E. Valero, A. Sivanathan, F. Bosche, M. Abdel-Wahab, Musculoskeletal disorders in construction: A review and a novel system for activity tracking with body area network, Applied Ergonomics. 54 (2016), pp. 120-130, https://doi.org/10.1016/j.apergo.2015.11.020.
[41] J.Y. Chen, J. Qiu, C.B. Ahn, Construction worker's awkward posture recognition through supervised motion tensor decomposition, Automation in Construction. 77 (2017), pp. 67-81, https://doi.org/10.1016/j.autcon.2017.01.020.
[42] H. Kim, C.R. Ahn, K. Yang, Identifying safety hazards using collective bodily responses of workers, Journal of Construction Engineering and Management. 143 (2) (2017), pp. 04016090, https://doi.org/10.1061/(asce)co.1943-7862.0001220.
[43] Y.C. Fang, R.J. Dzeng, Accelerometer-based fall-portent detection algorithm for construction tiling operation, Automation in Construction. 84 (2017), pp. 214-230, https://doi.org/10.1016/j.autcon.2017.09.015.
[44] M.F. Antwi-Afari, Y. Qarout, R. Herzallah, S. Anwer, W. Umer, Y. Zhang, P. Manu, Deep learning-based networks for automated recognition and classification of awkward working postures in construction using wearable insole sensor data, Automation in Construction. 136 (2022), pp. 104181, https://doi.org/10.1016/j.autcon.2022.104181.
[45] Y. Gong, K. Yang, J. Seo, J.G. Lee, Wearable acceleration-based action recognition for long-term and continuous

activity analysis in construction site, Journal of Building Engineering. 52 (2022), pp. 104448, https://doi.org/10.1016/j.jobe.2022.104448.
[46] J.Q. Zhao, E. Obonyo, Applying incremental deep neural networks-based posture recognition model for ergonomics risk assessment in construction, Advanced Engineering Informatics. 50 (2021), pp. 101374, https://doi.org/10.1016/j.aei.2021.101374.
[47] P. Spielholz, B. Silverstein, M. Morgan, H. Checkoway, J. Kaufman, Comparison of self-report, video observation and direct measurement methods for upper extremity musculoskeletal disorder physical risk factors, Ergonomics. 44 (6) (2001), pp. 588-613, https://doi.org/10.1080/00140130118050.
[48] S. Hignett, L. McAtamney, Rapid entire body assessment (REBA), Applied Ergonomics. 31 (2) (2000), pp. 201-205, https://doi.org/10.1016/s0003-6870(99)00039-3.
[49] G.C. David, Ergonomic methods for assessing exposure to risk factors for work-related musculoskeletal disorders, Occupational medicine. 55 (3) (2005), pp. 190-199, https://doi.org/10.1093/occmed/kqi082.
[50] I. Awolusi, E. Marks, M. Hallowell, Wearable technology for personalized construction safety monitoring and trending: Review of applicable devices, Automation in Construction. 85 (2018), pp. 96-106, https://doi.org/10.1016/j.autcon.2017.10.010.
[51] W. Umer, H. Li, G.P.Y. Szeto, A.Y.L. Wong, Identification of biomechanical risk factors for the development of lower-back disorders during manual rebar tying, Journal of Construction Engineering and Management. 143 (1) (2017), pp. 04016080, https://doi.org/10.1061/(asce)co.1943-7862.0001208.
[52] M.F. Antwi-Afari, H. Li, W. Umer, Y. Yu, X. Xing, Construction activity recognition and ergonomic risk assessment using a wearable insole pressure system, Journal of Construction Engineering and Management. 146 (7) (2020), pp. 04020077, https://doi.org/10.1061/(asce)co.1943-7862.0001849.
[53] M.F. Antwi-Afari, S. Anwer, W. Umer, H.-Y. Mi, Y. Yu, S. Moon, M.U. Hossain, Machine learning-based identification and classification of physical fatigue levels: A novel method based on a wearable insole device, International Journal of Industrial Ergonomics. 93 (2023), pp. 103404, https://doi.org/10.1016/j.ergon.2022.103404.
[54] S.S. Bangaru, C. Wang, S.A. Busam, F. Aghazadeh, ANN-based automated scaffold builder activity recognition through wearable EMG and IMU sensors, Automation in Construction. 126 (2021), pp. 103653, https://doi.org/10.1016/j.autcon.2021.103653.
[55] J. Seo, S. Lee, Automated postural ergonomic risk assessment using vision-based posture classification, Automation in Construction. 128 (2021), pp. 103725, https://doi.org/10.1016/j.autcon.2021.103725.
[56] M. Jung, S. Chi, Human activity classification based on sound recognition and residual convolutional neural network, Automation in Construction. 114 (2020), pp. 103177, https://doi.org/10.1016/j.autcon.2020.103177.
[57] M.A. Khan, M. Sharif, T. Akram, M. Raza, T. Saba, A. Rehman, Hand-crafted and deep convolutional neural network features fusion and selection strategy: An application to intelligent human action recognition, Applied Soft Computing. 87 (2020), pp. 105986, https://doi.org/10.1016/j.asoc.2019.105986.
[58] C. Bontrup, W.R. Taylor, M. Fliesser, R. Visscher, T. Green, P.M. Wippert, R. Zemp, Low back pain and its relationship with sitting behaviour among sedentary office workers, Applied Ergonomics. 81 (2019), pp. 102894, https://doi.org/10.1016/j.apergo.2019.102894.
[59] M. Zhao, G. Beurier, H. Wang, X. Wang, Driver posture monitoring in highly automated vehicles using pressure measurement, Traffic injury prevention. 22 (4) (2021), pp. 278-283, https://doi.org/10.1080/15389588.2021.1892087.
[60] A. Behera, Z. Wharton, A. Keidel, B. Debnath, Deep CNN, body pose, and body-object interaction features for drivers' activity monitoring, IEEE Transactions on Intelligent Transportation Systems. 23 (3) (2022), pp. 2874-2881, https://doi.org/10.1109/tits.2020.3027240.
[61] X.Y. Zhang, J.M. Fan, T. Peng, P. Zheng, C.K.M. Lee, R.Z. Tang, A privacy-preserving and unobtrusive sitting posture recognition system via pressure array sensor and infrared array sensor for office workers, Advanced Engineering Informatics. 53 (2022), pp. 101690, https://doi.org/10.1016/j.aei.2022.101690.

[62] L. Su, C. Sun, D. Cao, A. Khajepour, Efficient driver anomaly detection via conditional temporal proposal and classification network, IEEE Transactions on Computational Social Systems. 10 (2) (2023), pp. 736-745, https://doi.org/10.1109/tcss.2022.3158480.
[63] C. Ou, F. Karray, Enhancing driver distraction recognition using generative adversarial networks, IEEE Transactions on Intelligent Vehicles. 5 (3) (2020), pp. 385-396, https://doi.org/10.1109/tiv.2019.2960930.
[64] V. Balasubramanian, M. Jagannath, Detecting motorcycle rider local physical fatigue and discomfort using surface electromyography and seat interface pressure, Transportation Research Part F: Traffic Psychology and Behaviour. 22 (2014), pp. 150-158, https://doi.org/10.1016/j.trf.2013.12.010.
[65] M. Lu, X. Lu, Keypoint-enhanced adaptive weighting model with effective frequency channel attention for driver action recognition, Engineering Applications of Artificial Intelligence. 123 (2023), pp. 106321, https://doi.org/10.1016/j.engappai.2023.106321.
[66] C. Ma, W. Li, R. Gravina, J. Cao, Q. Li, G. Fortino, Activity level assessment using a smart cushion for people with a sedentary lifestyle, Sensors. 17 (10) (2017), pp. 2269, https://doi.org/10.3390/s17102269.
[67] B. Schwartz, J.M. Kapellusch, A. Schrempf, K. Probst, M. Haller, A. Baca, Effect of alternating postures on cognitive performance for healthy people performing sedentary work, Ergonomics. 61 (6) (2018), pp. 778-795, https://doi.org/10.1080/00140139.2017.1417642.
[68] C. Wilkes, R. Kydd, M. Sagar, E. Broadbent, Upright posture improves affect and fatigue in people with depressive symptoms, Journal of Behavior Therapy and Experimental Psychiatry. 54 (2017), pp. 143-149, https://doi.org/10.1016/j.jbtep.2016.07.015.
[69] J. Li, H. Li, F. Wang, A.S.K. Cheng, X. Yang, H. Wang, Proactive analysis of construction equipment operators' hazard perception error based on cognitive modeling and a dynamic Bayesian network, Reliability Engineering & System Safety. 205 (2021), pp. 107203, https://doi.org/10.1016/j.ress.2020.107203.
[70] J. Li, H. Li, W. Umer, H. Wang, X. Xing, S. Zhao, J. Hou, Identification and classification of construction equipment operators' mental fatigue using wearable eye-tracking technology, Automation in Construction. 109 (2020), pp. 103000, https://doi.org/10.1016/j.autcon.2019.103000.
[71] N.D. Nath, T. Chaspari, A.H. Behzadan, Automated ergonomic risk monitoring using body-mounted sensors and machine learning, Advanced Engineering Informatics. 38 (2018), pp. 514-526, https://doi.org/10.1016/j.aei.2018.08.020.
[72] D. Ren-Jye, H. Hsien, W. Keisuke, Applications of ICTs and action recognition for construction workers, Trends in Civil Engineering and its Architecture. 1 (3) (2018), pp. 48-54, https://doi.org/10.32474/TCEIA.2018.01.000113.
[73] B. Li, B.X. Bai, C. Han, Upper body motion recognition based on key frame and random forest regression, Multimedia Tools and Applications. 79 (7-8) (2020), pp. 5197-5212, https://doi.org/10.1007/s11042-018-6357-y.
[74] A. Kulikajevas, R. Maskeliunas, R. Damasevicius, Detection of sitting posture using hierarchical image composition and deep learning, PEERJ Computer Science. (2021), pp. 20, https://doi.org/10.7717/peerj-cs.442.
[75] M.Y. Li, Z.H. Jiang, Y.T. Liu, S.H. Chen, M. Wozniak, R. Scherer, R. Damasevicius, W. Wei, Z.Y. Li, Z.X. Li, Sitsen: Passive sitting posture sensing based on wireless devices, International Journal of Distributed Sensor Networks. 17 (7) (2021), pp. 1-11, https://doi.org/10.1177/15501477211024846.
[76] R. Gravina, Q. Li, Emotion-relevant activity recognition based on smart cushion using multi-sensor fusion, Information Fusion. 48 (2019), pp. 1-10, https://doi.org/10.1016/j.inffus.2018.08.001.
[77] X. Ran, C. Wang, Y. Xiao, X.L. Gao, Z.Y. Zhu, B. Chen, A portable sitting posture monitoring system based on a pressure sensor array and machine learning, Sensors and Actuators A-Physical. 331 (2021), pp. 1-10, https://doi.org/10.1016/j.sna.2021.112900.
[78] D.E. Gyi, J.M. Porter, Interface pressure and the prediction of car seat discomfort, Applied Ergonomics. 30 (2) (1999), pp. 99-107, https://doi.org/10.1016/s0003-6870(98)00018-0.
[79] V. Leos-Barajas, T. Photopoulou, R. Langrock, T.A. Patterson, Y.Y. Watanabe, M. Murgatroyd, Y.P. Papastamatiou,

R.B. O'Hara, Analysis of animal accelerometer data using hidden Markov models, Methods in Ecology and Evolution. 8 (2) (2016), pp. 161-173, https://doi.org/10.1111/2041-210x.12657.

[80] K.T. Sweeney, T.E. Ward, S.F. McLoone, Artifact removal in physiological signals--practices and possibilities, IEEE Transactions on Information Technology in Biomedicine. 16 (3) (2012), pp. 488-500, https://doi.org/10.1109/TITB.2012.2188536.

[81] B.O. Akinnuli, O.A. Dahunsi, S.P. Ayodeji, O.P. Bodunde, Z. Jin, Whole-body vibration exposure on earthmoving equipment operators in construction industries, Cogent Engineering. 5 (1) (2018), pp. 1507266, https://doi.org/10.1080/23311916.2018.1507266.

[82] V. Korakakis, K. O'Sullivan, R. Whiteley, P.B. O'Sullivan, A. Korakaki, A. Kotsifaki, P.V. Tsaklis, A. Tsiokanos, G. Giakas, Notions of "optimal" posture are loaded with meaning. Perceptions of sitting posture among asymptomatic members of the community, Musculoskeletal Science and Practice. 51 (2021), pp. 102310, https://doi.org/10.1016/j.msksp.2020.102310.

[83] Q.S. Hu, X.C. Tang, W. Tang, A smart chair sitting posture recognition system using flex sensors and FPGA implemented artificial neural network, IEEE Sensors Journal. 20 (14) (2020), pp. 8007-8016, https://doi.org/10.1109/jsen.2020.2980207.

[84] H.S. Woo, J.C. Oh, S.Y. Won, Effects of asymmetric sitting on spinal balance, Journal of Physical Therapy Science. 28 (2) (2016), pp. 355-359, https://doi.org/10.1589/jpts.28.355.

[85] Shenzhen LEGACT Technology Co., Ltd. https://film-sensor.com/force-sensing-technology/. Accessed date: May 2023.

[86] WitMotion Shenzhen Co., Ltd. https://www.wit-motion.com/. Accessed date: May 2023.

[87] J. Xu, E.B. Song, Y.T. Luo, Y.M. Zhu, Optimal distributed kalman filtering fusion algorithm without invertibility of estimation error and sensor noise covariances, IEEE Signal Processing Letters. 19 (1) (2012), pp. 55-58, https://doi.org/10.1109/lsp.2011.2177495.

[88] B. Das, S. Gangopadhyay, An ergonomics evaluation of posture related discomfort and occupational health problems among rice farmers, Occupational Ergonomics. 10 (1-2) (2011), pp. 25-38, https://content.iospress.com/articles/occupational-ergonomics/oer00190.

[89] M. Pau, B. Leban, P. Fadda, G. Fancello, M.A. Nussbaum, Effect of prolonged sitting on body-seat contact pressures among quay crane operators: A pilot study, Work. 55 (3) (2016), pp. 605-611, https://doi.org/10.3233/WOR-162434.

[90] B. Leban, G. Fancello, P. Fadda, M. Pau, Changes in trunk sway of quay crane operators during work shift: A possible marker for fatigue?, Applied Ergonomics. 65 (2017), pp. 105-111, https://doi.org/10.1016/j.apergo.2017.06.007.

[91] M. Makhsous, F. Lin, J. Bankard, R.W. Hendrix, M. Hepler, J. Press, Biomechanical effects of sitting with adjustable ischial and lumbar support on occupational low back pain: evaluation of sitting load and back muscle activity, BMC Musculoskeletal Disorders. 10 (2009), pp. 1-11, https://doi.org/10.1186/1471-2474-10-17.

[92] Y.H. Qin, Y.Y. Yan, H.Q. Ji, Y.Q. Wang, Recursive correlative statistical analysis method with sliding windows for incipient fault detection, IEEE Transactions on Industrial Electronics. 69 (4) (2022), pp. 4185-4194, https://doi.org/10.1109/tie.2021.3070521.

[93] J. Ryu, J. Seo, H. Jebelli, S. Lee, Automated action recognition using an accelerometer-embedded wristband-type activity tracker, Journal of Construction Engineering and Management. 145 (1) (2019), pp. 04018114, https://doi.org/10.1061/(asce)co.1943-7862.0001579.

[94] S.J. Preece, J.Y. Goulermas, L.P.J. Kenney, D. Howard, K. Meijer, R. Crompton, Activity identification using body-mounted sensors-a review of classification techniques, Physiological Measurement. 30 (4) (2009), pp. R1-R33, https://doi.org/10.1088/0967-3334/30/4/r01.

[95] Y.J. Liu, M.J. Yu, G.Z. Zhao, J.J. Song, Y. Ge, Y.C. Shi, Real-time movie-induced discrete emotion recognition from eeg signals, IEEE Transactions on Affective Computing. 9 (4) (2018), pp. 550-562, https://doi.org/10.1109/taffc.2017.2660485.

[96] Z.M. Hira, D.F. Gillies, A review of feature selection and feature extraction methods applied on microarray data, Advances in bioinformatics. 2015 (1) (2015), pp. 1-13, https://doi.org/10.1155/2015/198363.
[97] C. Janiesch, P. Zschech, K. Heinrich, Machine learning and deep learning, Electronic Markets. 31 (3) (2021), pp. 685-695, https://doi.org/10.1007/s12525-021-00475-2.
[98] R. Akhavian, A.H. Behzadan, Smartphone-based construction workers' activity recognition and classification, Automation in Construction. 71 (2016), pp. 198-209, https://doi.org/10.1016/j.autcon.2016.08.015.
[99] L. Bao, S.S. Intille, Activity recognition from user-annotated acceleration data, International Conference on Pervasive Computing, Vienna, Austria, April 21-23, 2004, pp. 1-17, https://doi.org/10.1007/978-3-540-24646-6_1.
[100] A. Logacjov, K. Bach, A. Kongsvold, H.B. Bardstu, P.J. Mork, HARTH: A human activity recognition dataset for machine learning, Sensors. 21 (23) (2021), https://doi.org/10.3390/s21237853.
[101] J. Roh, H.J. Park, K.J. Lee, J. Hyeong, S. Kim, B. Lee, Sitting posture monitoring system based on a low-cost load cell using machine learning, Sensors. 18 (1) (2018), https://doi.org/10.3390/s18010208.
[102] Y. Bengio, Deep learning of representations: Looking forward, Statistical Language and Speech Processing: First International Conference, Tarragona, Spain, July 29-31, 2013, pp. 1-37, https://doi.org/10.1007/978-3-642-39593-2_1.
[103] Z.L. Wang, D.H. Wu, J.M. Chen, A. Ghoneim, M.A. Hossain, A triaxial accelerometer-based human activity recognition via EEMD-based features and game-theory-based feature selection, IEEE Sensors Journal. 16 (9) (2016), pp. 3198-3207, https://doi.org/10.1109/jsen.2016.2519679.
[104] D. Ravi, C. Wong, B. Lo, G.Z. Yang, A deep learning approach to on-node sensor data analytics for mobile or wearable devices, IEEE Journal of Biomedical and Health Informatics. 21 (1) (2017), pp. 56-64, https://doi.org/10.1109/jbhi.2016.2633287.
[105] Y. LeCun, Y. Bengio, G. Hinton, Deep learning, Nature. 521 (7553) (2015), pp. 436-444, https://doi.org/10.1038/nature14539.
[106] M.F. Antwi-Afari, H. Li, Y.T. Yu, L.L. Kong, Wearable insole pressure system for automated detection and classification of awkward working postures in construction workers, Automation in Construction. 96 (2018), pp. 433-441, https://doi.org/10.1016/j.autcon.2018.10.004.
[107] S.B. Kotsiantis, Decision trees: A recent overview, Artificial Intelligence Review. 39 (4) (2013), pp. 261-283, https://doi.org/10.1007/s10462-011-9272-4.
[108] Z.H. Wang, Z.C. Yang, T. Dong, A review of wearable technologies for elderly care that can accurately track indoor position, recognize physical activities and monitor vital signs in real time, Sensors. 17 (2) (2017), pp. 341, https://doi.org/10.3390/s17020341.
[109] F. Attal, S. Mohammed, M. Dedabrishvili, F. Chamroukhi, L. Oukhellou, Y. Amirat, Physical human activity recognition using wearable sensors, Sensors. 15 (12) (2015), pp. 31314-31338, https://doi.org/10.3390/s151229858.
[110] J. Ahmad, H. Andersson, J. Siden, Screen-printed piezoresistive sensors for monitoring pressure distribution in wheelchair, IEEE Sensors Journal. 19 (6) (2019), pp. 2055-2063, https://doi.org/10.1109/jsen.2018.2885638.
[111] J. Ahmad, J. Siden, H. Andersson, A proposal of implementation of sitting posture monitoring system for wheelchair utilizing machine learning methods, Sensors. 21 (19) (2021), pp. 6349, https://doi.org/10.3390/s21196349.
[112] F. Shahid, A. Zameer, M. Muneeb, Predictions for COVID-19 with deep learning models of LSTM, GRU and Bi-LSTM, Chaos Solitons & Fractals. 140 (2020), pp. 1-9, https://doi.org/10.1016/j.chaos.2020.110212.
[113] R. Yan, J.Q. Liao, J. Yang, W. Sun, M.Y. Nong, F.P. Li, Multi-hour and multi-site air quality index forecasting in Beijing using CNN, LSTM, CNN-LSTM, and spatiotemporal clustering, Expert Systems with Applications. 169 (2021), pp. 114513, https://doi.org/10.1016/j.eswa.2020.114513.
[114] S. Gao, Y.F. Huang, S. Zhang, J.C. Han, G.Q. Wang, M.X. Zhang, Q.S. Lin, Short-term runoff prediction with GRU and LSTM networks without requiring time step optimization during sample generation, Journal of Hydrology. 589 (2020), pp. 125188, https://doi.org/10.1016/j.jhydrol.2020.125188.

[115] C. Park, C. Lee, L. Hong, Y. Hwang, T. Yoo, J. Tang, Y. Hone, K.H. Bae, H.K. Kim, S-2-Net: Machine reading comprehension with SRU-based self-matching networks, ETRI Journal. 41 (3) (2019), pp. 371-382, https://doi.org/10.4218/etrij.2017-0279.

[116] F. Luna-Perejon, J.M. Montes-Sanchez, L. Duran-Lopez, A. Vazquez-Baeza, I. Beasley-Bohorquez, J.L. Sevillano-Ramos, IoT device for sitting posture classification using artificial neural networks, Electronics. 10 (15) (2021), https://doi.org/10.3390/electronics10151825.

[117] N. Srivastava, G. Hinton, A. Krizhevsky, I. Sutskever, R. Salakhutdinov, Dropout: A simple way to prevent neural networks from overfitting, Journal of Machine Learning Research. 15 (2014), pp. 1929-1958, ISSN: 1533-7928.

[118] K. Koc, Ö. Ekmekcioğlu, A.P. Gurgun, Prediction of construction accident outcomes based on an imbalanced dataset through integrated resampling techniques and machine learning methods, Engineering, Construction and Architectural Management. 30 (9) (2022), pp. 4486-4517, https://doi.org/10.1108/ecam-04-2022-0305.

[119] C. Chen, Z.H. Zhu, A. Hammad, Automated excavators activity recognition and productivity analysis from construction site surveillance videos, Automation in Construction. 110 (2020), pp. 103045, https://doi.org/10.1016/j.autcon.2019.103045.

[120] C. Chen, Z.H. Zhu, A. Hammad, M. Akbarzadeh, Automatic identification of idling reasons in excavation operations based on excavator-truck relationships, Journal of Computing in Civil Engineering. 35 (5) (2021), pp. 04021015, https://doi.org/10.1061/(asce)cp.1943-5487.0000981.

[121] J. Kim, S. Chi, J. Seo, Interaction analysis for vision-based activity identification of earthmoving excavators and dump trucks, Automation in Construction. 87 (2018), pp. 297-308, https://doi.org/10.1016/j.autcon.2017.12.016.

[122] K.M. Rashid, J. Louis, Times-series data augmentation and deep learning for construction equipment activity recognition, Advanced Engineering Informatics. 42 (2019), pp. 100944, https://doi.org/10.1016/j.aei.2019.100944.